Molecular Fe, CO and Ni carbide carbonyl clusters and Nanoclusters†

Molecular Fe, Co and Ni Carbide Carbonyl Clusters and Nanoclusters[†]

Cristiana Cesari, Cristina Femoni, Maria Carmela Iapalucci, Stefano Zacchini*

Dipartimento di Chimica Industriale "Toso Montanari", Università di Bologna, Viale Risorgimento 4 - 40136 Bologna, Italy. E-mail: stefano.zacchini@unibo.it

Abstract: The present minireview highlights the work of our group on Fe, Co and Ni carbide carbonyl clusters and nanoclusters, placing it in the context of the recent literature. After a brief introduction, Section 2 gives a short summary on the general features of molecular carbide carbonyl clusters. Then, specific examples of Fe, Co and Ni carbide carbonyl clusters are presented in the following three Sections. Each Section includes both homometallic and heterometallic clusters, as well as discussion of some of their most relevant chemical, electrochemical, structural and physical properties. General conclusions are outlined in Section 6.

[†] Dedicated to Professor Guido Pampaloni on occasion of his retirement, and in recognition of his contribution to coordination and organometallic chemistry.

Keywords: Cluster compounds; Carbonyl ligands; Carbide; Molecular nanoclusters; Nanochemistry

1. Introduction

The square-pyramidal $Fe_5C(CO)_{15}$ species, containing a semi-exposed C-atom, was the first structurally characterized metal carbide carbonyl cluster [1]. Soon after, the structure of the octahedral $Ru_6C(CO)_{17}$ cluster was unravelled by single crystal X-ray diffraction (SC-XRD), showing the presence of a fully interstitial carbide atom [2,3]. Several other metal carbide carbonyl clusters were, then, discovered including both homometallic and heterometallic species, as well as mono-carbide, poly-carbide, mono-acetylide and poly-acetylide species [4-11]. The term "acetylide" is used to indicate species that contain tightly bonded C_2-units.

Clusters containing semi-exposed carbide atoms, such as $Fe_5C(CO)_{15}$, attracted a great interest mainly focused in the reactivity of the semi-exposed C-atom [12-18]. Indeed, this can be exploited for the formation of C-H and C-C bonds, and serves as model for carbide atoms on metal surfaces. These studies widely contributed to the development of the cluster surface analogy [19,20]. Moreover, semi-exposed carbides in molecular clusters helped the understanding of relevant industrial processes, such as the Fischer-Tropsch reaction [21-29].

From the other side, fully interstitial carbide atoms are not accessible to reagents, and display a limited (or almost null) direct reactivity. Nonetheless, they play a fundamental role in the stabilisation of metal carbonyl clusters in two synergic ways [30,31]:

(a) Formation of additional M-C bonds, which add to M-M ones, reinforces the metal cage of the cluster. This point is rather important in the case of first raw transition metals, such as Fe, Co and Ni, since their M-M bonds are considerably weaker than those involving second and third raw transition metals, such as Ru, Os, Rh, Ir and Pt.

(b) Interstitial carbides act as internal ligands lowering the number of surface CO ligands and, thus, reducing steric problems. To exemplify this point, ruthenium forms the octahedral non-carbide cluster $[Ru_6(CO)_{18}]^{2-}$ [32] as well as the octahedral carbide $[Ru_6C(CO)_{16}]^{2-}$ [33]. Conversely, in the case of iron, only the carbide $[Fe_6C(CO)_{16}]^{2-}$ is known [34]. This is due to the fact that Fe is smaller than Ru and, therefore, there is no space on the surface of a Fe_6 octahedron for 18 CO ligands.

As the major result of these stabilising effects, Fe, Co and Ni carbide carbonyl clusters systematically reach higher nuclearities than species containing only carbonyl ligands. Thus, the largest M-CO clusters (without any interstitial atom) display 4, 6 and 12 metal atoms for Fe, Co and Ni, respectively, whereas, including interstitial carbides, they can reach up to 6, 13 and 45 metal atoms. Indeed, $[Ni_{45}C_{10}(CO)_{46}]^{6-}$ represents the largest metal carbide carbonyl cluster reported to date, considering all transition metals [35]. Large molecular metal carbide carbonyl clusters are comparable in size to ultrasmall metal nanoparticles and atomically precise metal nanoclusters [36-39]. In addition, the enhanced stability conferred by the carbide atoms allows for a variety of chemical and electrochemical reactions on the surface of the cluster [40].

Metal carbide carbonyl clusters have recently attracted a renewed interest because of different factors. Firstly, the discovery that the active site of nitrogenase enzymes contains a Fe-S carbide cluster [41-46] generated some interest in Fe carbide carbonyl clusters [47-51]. In particular, several studies have been recently focused in the possibility of introducing S-atoms on Fe carbide carbonyl clusters [52,53]. Then, robust Fe and Co carbide carbonyl clusters have shown high performances as electrocatalysts for the hydrogen evolution reaction (HER) [54-57]. In addition, high nuclearity metal carbonyl clusters (MCCs) including larger carbide MCCs may be viewed as atomically precise metal nanoclusters and, therefore, contribute to nanochemistry [11,40,58,59].

Within this framework, the present minireview is mainly focused in highlighting the work of our group on Fe, Co and Ni carbide carbonyl clusters, placing it in the context of the recent literature. Thus, a general review on metal carbide carbonyl clusters is outside our scope, and general readings can be found in the references.

After this brief introduction, Section 2 will give a short summary on the general features of the species analyzed in this minireview. The following three Sections will present some examples of Fe (Section 3), Co (Section 4) and Ni (Section 5) carbide carbonyl clusters. General conclusions will be outlined in Section 6. The readers can find tables with the full list of the clusters mentioned in this mini-review, with pertinent references and CCDC codes, in the Supporting Information.

2. General Features

Metal carbide carbonyl clusters can be directly accessed following three general synthetic procedures [11,30,31,60]:

1) Thermal disproportionation of CO to C and CO_2, upon heating of simple metal carbonyls. This synthetic approach has been widely employed in the case of Re, Fe, Ru, and Os carbonyls.
2) CO splitting by the reduction of a bridging CO ligand. Coordination of a Lewis acid, such as RCO^+ (generated from RCOCl), to the O-atom of a bridging carbonyl results in a $[M_n]$–C–O–C(O)R species, which is, then, reduced to a metal carbide following elimination of $RCOO^-$. This approach can be applied for the synthesis of some Fe and Co carbide clusters.
3) Direct reaction of a metal carbonyl anion with carbon halides (*e.g.*, CCl_4, C_2Cl_4, C_2Cl_6, C_3Cl_6). This procedure has been largely employed for the synthesis of Co, Rh, and Ni carbide carbonyl clusters.

Once prepared, carbide carbonyl clusters can be further modified and transformed into new carbide clusters by means of all typical reactions of metal carbonyl clusters. These include thermal reactions, oxidation, reduction, redox condensation, reactions with Lewis acids and nucleophiles. Some examples will be given in the following sections [11,30,30,58,61,62].

From a structural point of view, the C-atoms can be isolated ("proper" carbide clusters) or form tightly bonded C_2 units (acetylide clusters). Even if it can be somehow misleading, the term carbide carbonyl cluster is often used in the literature in a general way to refer both to (proper, C isolated) carbide and acetylide clusters. Herein, the term "carbide" will be employed, as in the literature, to refer in a general way to clusters containing carbon atoms, either isolated or as C_2-units. Then, the term "isolated carbide" will be used whenever it will be needed to explicitly refer to clusters containing isolated C-atoms, whereas the term "acetlyde" cluster will be employed in the case of bonded C_2 units, regardless of the actual C-C distance and bond order. Within formulas, C_n (n = 1-10, for structurally characterized clusters) indicates n-isolated C-atoms, whereas $(C_2)_n$ (n = 1-4, for structurally characterized clusters) indicates n-C_2 units. It must be remarked that the term "acetylide" is used to indicate that the two C-atoms are covalently bonded, without a specification of the bond order. Indeed, the C-C bond distances in acetylide clusters span a wide range of values, comprising those of organic alkynes, alkenes and alkanes.

In the present minireview, the terms carbide and acetylide are used as in the case of extended transition metal carbides (e.g., TiC, WC, Fe_3C, Cr_3C_2) and not to indicate ionic carbides. Indeed, metal carbide carbonyl clusters contain (delocalized) covalent bonds and not ionic bonds.

Most of the clusters contain fully interstitial C-atoms (or C_2 units), even if some interesting examples of clusters displaying semi-interstitial (semi-exposed) carbide atoms are also known. Usually, C-atoms are included within octahedral, trigonal prismatic or square anti-prismatic metal cages, which can be further capped by metal atoms increasing the coordination number of the carbide atom. Selected examples of Fe, Co and Ni carbide carbonyl clusters mainly taken from our recent work will be described in the following Sections and compared to literature data.

3. Iron Carbide Carbonyl Clusters

3.1 Homometallic Iron Carbide Carbonyl Clusters

Iron carbide carbonyl clusters have been recently reviewed and, therefore, only a few relevant features will be herein outlined [4]. Based on their structures, homometallic iron carbide carbonyl clusters can be grouped into three main categories:

1) Fe_4C clusters with a butterfly structure which display a semi-exposed carbide (green in Scheme 1), such as $[Fe_4C(CO)_{13}]$ [63], $[Fe_4C(CO)_{12}]^{2-}$ [17], $[HFe_4C(CO)_{12}]^{-}$ [64], and $[HFe_4CH(CO)_{12}]$ [65];

2) Fe_5C clusters with a square-pyramidal structure which possess a basal semi-exposed carbide (blue in Scheme 1), such as $[Fe_5C(CO)_{15}]$ [1], and $[Fe_5C(CO)_{14}]^{2-}$ [66];

3) Fe_6C octahedral clusters incorporating a fully interstitial carbide atom (red in Scheme 1), such as $[Fe_6C(CO)_{16}]^{2-}$ [34], and $[Fe_6C(CO)_{15}]^{4-}$ [67].

Some Fe carbide carbonyl clusters can be directly accessed by thermal disproportionation of CO ligands. For instance, heating $Fe(CO)_5$ in quinoline above 160 °C results in $[Fe_6C(CO)_{16}]^{2-}$ [34], that can be, then, employed as starting material for the preparation of other clusters (Scheme 1). Alternatively, $[Fe_4C(CO)_{12}]^{2-}$ can be prepared by reduction induced CO splitting after activation of a bridging CO with a Lewis acid [60]. This is a two-step reaction where, first, $[Fe_4(CO)_{13}]^{2-}$ is reacted with CH_3COCl to yield $[Fe_4(CO)_{12}(COC(O)CH_3)]^{-}$; this is, then, reduced with Na to afford $[Fe_4C(CO)_{12}]^{2-}$.

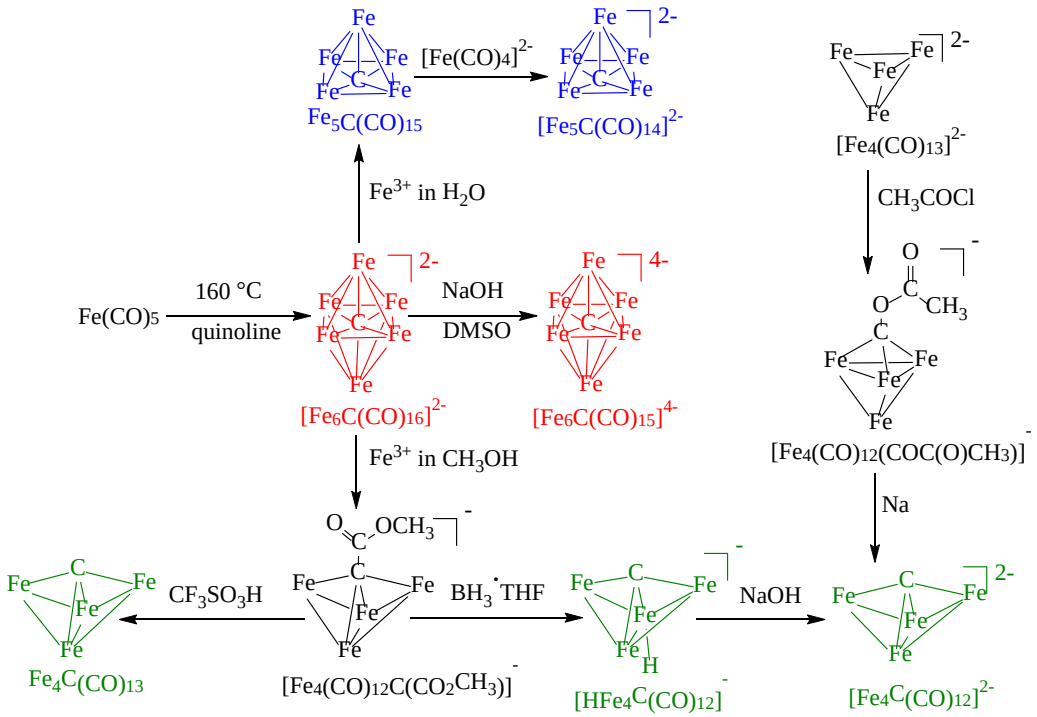

Scheme 1. Synthesis of Fe carbide carbonyl clusters. All the species have been isolated and fully characterized. $[Fe_6C(CO)_{16}]^{2-}$ is prepared directly from $Fe(CO)_5$ by thermal treatment. Other Fe carbide carbonyl clusters can be obtained from $[Fe_6C(CO)_{16}]^{2-}$ using redox reactions. Alternatively, $[Fe_4C(CO)_{12}]^{2-}$ can be prepared starting from $[Fe_4(CO)_{13}]^{2-}$ in a two-step reaction by CO scission. CO ligands have been omitted for clarity. Reproduced with permission from ref. 11.

The highly reduced cluster $[Fe_6C(CO)_{15}]^{4-}$ can be obtained from the reaction of $[Fe_6C(CO)_{16}]^{2-}$ with NaOH in DMSO or using Na/naphthalene in THF [67]. The former synthesis represents a typical reaction of metal carbonyls, that is, OH^- nucleophilic attack at a CO ligand followed by CO_2 elimination and deprotonation (Figure 1). The $[HFe_6C(CO)_{15}]^{3-}$ hydride has been identified by ^1H NMR spectroscopy during the protonation of $[Fe_6C(CO)_{15}]^{4-}$ with $HBF_4{\cdot}Et_2O$. The fact that $[Fe_6C(CO)_{15}]^{4-}$ is a base is further confirmed by its reaction with $Au(PPh_3)Cl$ which resulted in the bis-aurated species $[Fe_6C(CO)_{15}(AuPPh_3)_2]^{2-}$.

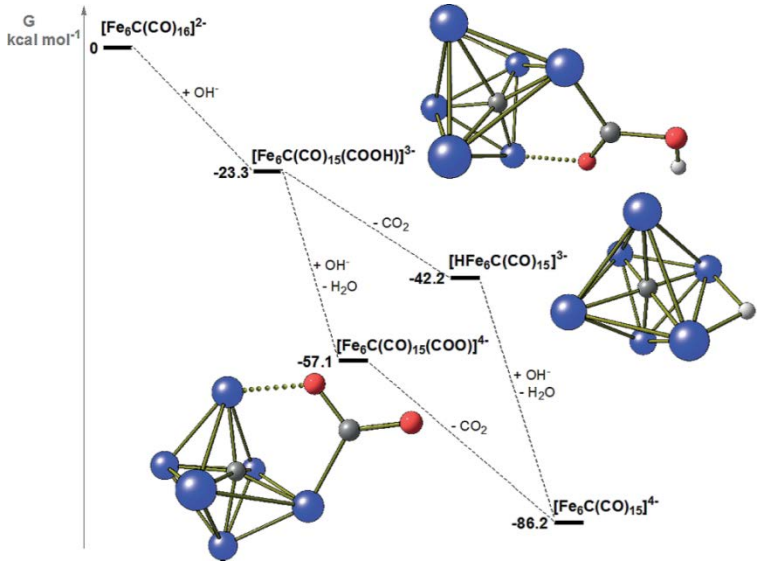

Fig. 1. Relative Gibbs energy values (kcal mol^{-1}) of reactants, products and intermediate species for the reaction $[Fe_6C(CO)_{16}]^{2-} + 2OH^- \rightarrow [Fe_6C(CO)_{15}]^{4-} + CO_2 + H_2O$. The DFT-optimized geometries of the intermediate species are reported. Ancillary carbonyl ligands have been omitted for clarity. C-PCM-ωB97X calculations. Color legend: Fe, blue; C, grey; O, red; H, white. Reproduced with permission from ref. 67.

Iron carbide carbonyl clusters are very important from a historical point of view. The square-pyramidal $[Fe_5C(CO)_{15}]$ was the first metal carbonyl cluster containing a carbide atom which was structurally characterized [1]. The study of the structures and reactivities of Fe carbide clusters mostly contributed to the development of the cluster-surface analogy and Fisher-Tropsch chemistry [19-29]. Indeed, Fe-C-CO clusters undergo reactions such as reduction, oxidation, fragmentation, protonation, hydrogenation, and alkylation, that in some cases afford new C-H and C-C bonds.

3.2 Iron Carbide Carbonyl Clusters containing Sulphur

A renewed interest for Fe carbide carbonyl clusters recently arose because of their relevance to nitrogenase chemistry [41-46]. Indeed, since an iron-sulfide-carbide cluster was found in the active site of the FeMoco cofactor of nitrogenase, the so called "carbide problem" became of paramount importance in bioinorganic chemistry. Some possible approach for the preparation of Fe-S-carbide clusters involve the use of $[Fe_6C(CO)_{16}]^{2-}$ as starting material [47-53]. The octahedral cluster, $[Fe_6C(CO)_{14}(S)]^{2-}$, containing one carbide and one sulfide can be obtained in a multistep synthesis (Scheme 2) [53]: 1) substitution of one CO ligand of $[Fe_6C(CO)_{16}]^{2-}$ with SO_2 to form $[Fe_6C(CO)_{15}(SO_2)]^{2-}$; 2) methylation of the latter with CF_3SO_3Me to give $[Fe_6C(CO)_{15}(SO_2Me)]^-$; 3) reduction to $[Fe_6C(CO)_{14}(S)]^{2-}$.

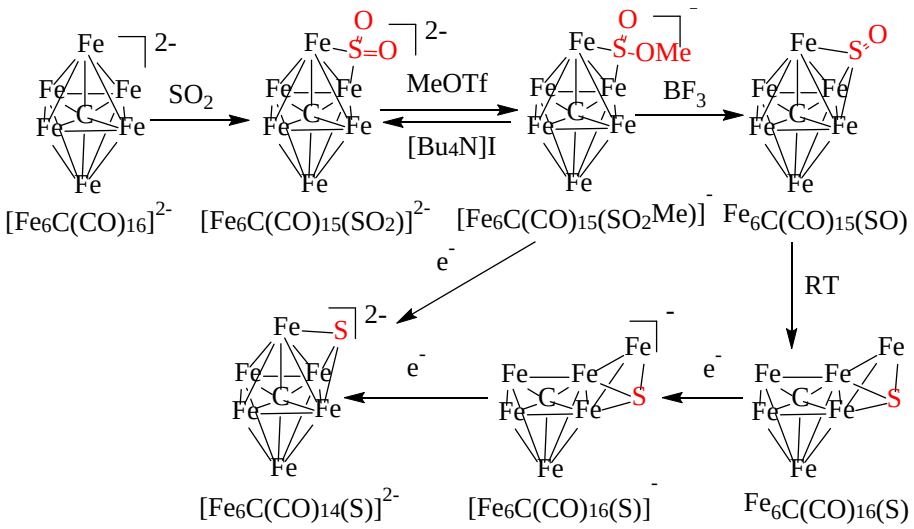

Scheme 2. Synthesis of $Fe_6C(CO)_{16}(S)$ and $[Fe_6C(CO)_{14}(S)]^{2-}$. $[Fe_6C(CO)_{16}]^{2-}$ is transformed into $[Fe_6C(CO)_{15}(SO_2)]^{2-}$ by CO substitution with SO_2. Further reactions with MeOTf, BF_3 and reduction with Na/naphthalene result in the target compounds. CO ligands have been omitted for clarity. Reproduced with permission from ref. 11.

Alternatively, the direct reaction of $[Fe_6C(CO)_{16}]^{2-}$ with S_2Cl_2 or S_8 affords mixtures of clusters, among which the μ_4-S^{2-} bridged μ_5,μ_6-bis(carbide) cluster $[\{Fe_5(\mu_5\text{-}C)(CO)_{13}\}\{Fe_6(\mu_6\text{-}C)(CO)_{15}\}(\mu_4\text{-}S)]^{2-}$ and the symmetric μ_4-S^{2-} bridged μ_5,μ_5-bis(carbide) cluster $[\{Fe_5(\mu_5\text{-}C)(CO)_{13}\}_2(\mu_4\text{-}S)]^{2-}$ clusters have been isolated (Figure 2) [47].

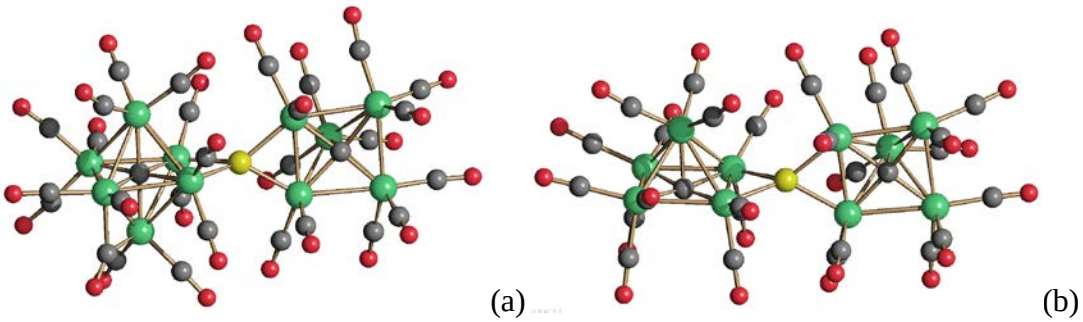

Fig. 2. Molecular structures of (a) $[\{Fe_5(\mu_5\text{-}C)(CO)_{13}\}\{Fe_6(\mu_6\text{-}C)(CO)_{15}\}(\mu_4\text{-}S)]^{2-}$ and (b) $[\{Fe_5(\mu_5\text{-}C)(CO)_{13}\}_2(\mu_4\text{-}S)]^{2-}$ (green, Fe; yellow, S; red, O; grey, C)

3.3 Heterometallic Iron Carbide Carbonyl Clusters

Several heterometallic Fe-based carbide carbonyl clusters can be prepared from the reactions of preformed Fe-carbide carbonyls with metal salts or complexes [18]. For instance, the reaction of $[Fe_5C(CO)_{14}]^{2-}$ with $[Mo(CO)_3(chpt)]$ (chpt = cycloheptatriene) affords the heterometallic carbide

$[Fe_5MoC(CO)_{17}]^{2-}$, which displays selective alkyne reduction [49,50]. Reaction of $[Fe_6C(CO)_{16}]^{2-}$ with $[Cu(MeCN)_4][BF_4]$ in refluxing THF results in the octahedral Fe-Cu carbide cluster $[Fe_4C(CO)_{12}\{Cu(MeCN)\}_2]$. Due to the lability of the Cu-bonded MeCN ligands, these can be easily replaced by halides, N-, O-, P-, S- and H-donor ligands affording a large variety of heteroleptic clusters containing the Fe_4Cu_2C core (Scheme 3) [68-72].

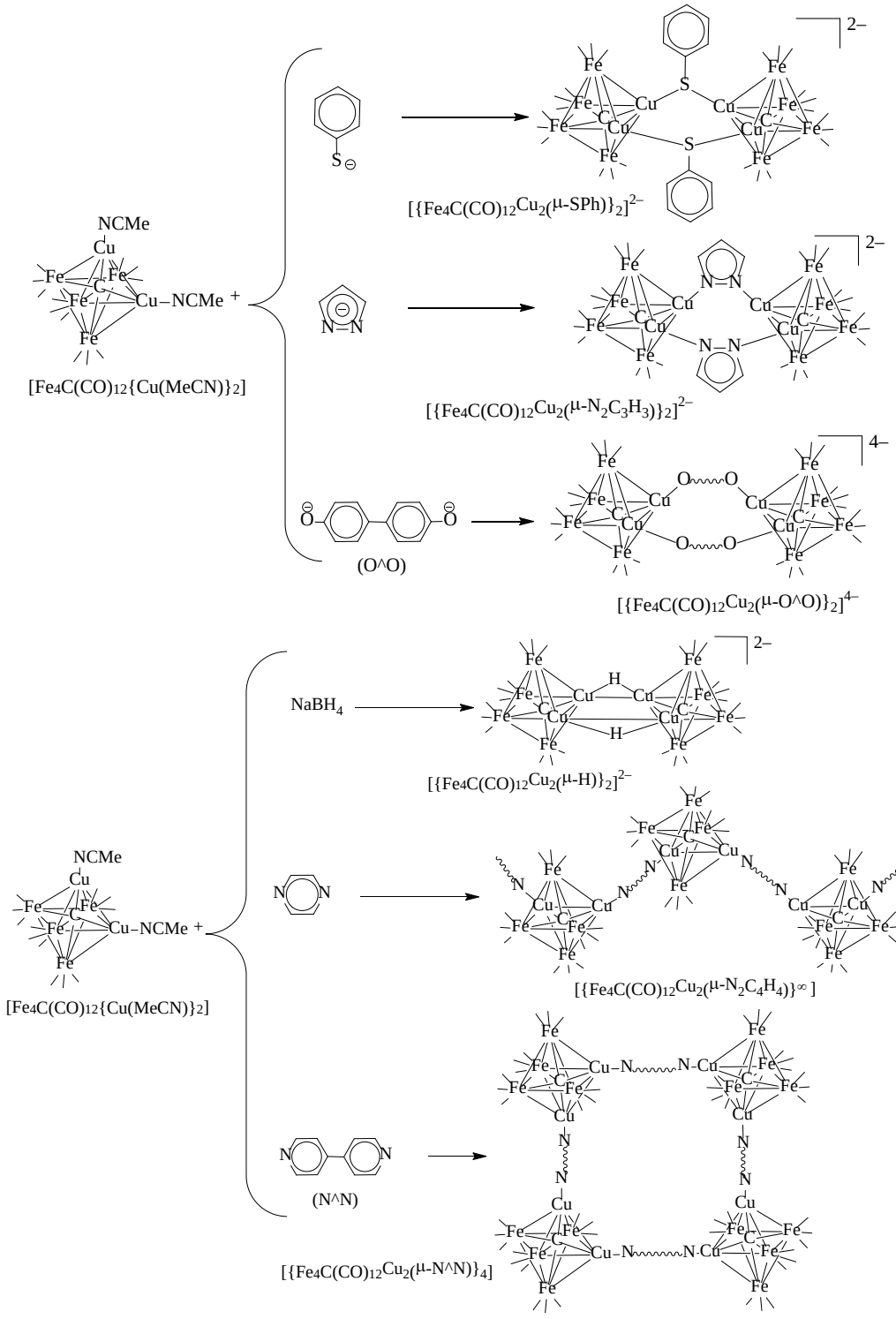

Scheme 3. Some representative reactions of $[Fe_4C(CO)_{12}\{Cu(MeCN)\}_2]$. Reproduced with permission from ref. 68.

Due to the enhanced stability conferred by the carbide atom, Fe carbide carbonyl clusters have been recently applied as electrocatalysts for the hydrogen evolution reaction (HER) [56,57]. In particular, $[Fe_4C(CO)_{12}]^{2-}$ displays a concerted proton-electron transfer mechanism under electrochemical control to form $[HFe_4C(CO)_{12}]^{2-}$, which is selective for HER also in the presence of CO_2. It is noteworthy that the isoelectronic and isostructural $[Fe_4N(CO)_{12}]^{-}$ features sequential electron and proton transfer reactions under the same electrochemical conditions and, in the presence of CO_2, affords formate via electrocatalytic CO_2 reduction rather than HER [73-77].

4. Cobalt Carbide Carbonyl Clusters

4.1 Homometallic Cobalt Carbide Carbonyl Clusters

The number of structurally characterized homometallic Co carbide carbonyl clusters is greater than Fe ones. Their nuclearity ranges from 6 to 13 Co atoms and they may contain one or two isolated carbide atoms as well as one tightly bonded C_2-acetylide unit [78-82]. The most straightforward synthesis of Co carbonyl carbides involves the use of carbon halides. Thus, refluxing $Co_2(CO)_8$ in neat CCl_4 affords the chloro-alkylidyne $Co_3(\mu_3\text{-}CCl)(CO)_9$ which, in turn, reacts with 3 equivalents of $[Co(CO)_4]^{-}$ resulting in the trigonal prismatic cluster $[Co_6C(CO)_{15}]^{2-}$. The latter can be alternatively obtained from the reaction of CCl_4 with six equivalents of $[Co(CO)_4]^{-}$. The paramagnetic $[Co_6C(CO)_{14}]^{-}$ cluster can be prepared in different ways: 1) oxidation of $[Co_6C(CO)_{15}]^{2-}$; 2) reaction of $Co_3(\mu_3\text{-}CCl)(CO)_9$ with 2 equivalents of $[Co(CO)_4]^{-}$; 3) reaction of $[Co_6(CO)_{15}]^{2-}$ with MeCOCl *via* CO scission induced by the addition of $MeCO^{+}$ to a coordinated CO ligand.

The mono-carbide $[Co_6C(CO)_{15}]^{2-}$ can be used as starting material for the preparation of several other homometallic Co carbide carbonyl clusters, by means of thermal reactions, redox condensation, oxidation and reduction (Scheme 4) [78].

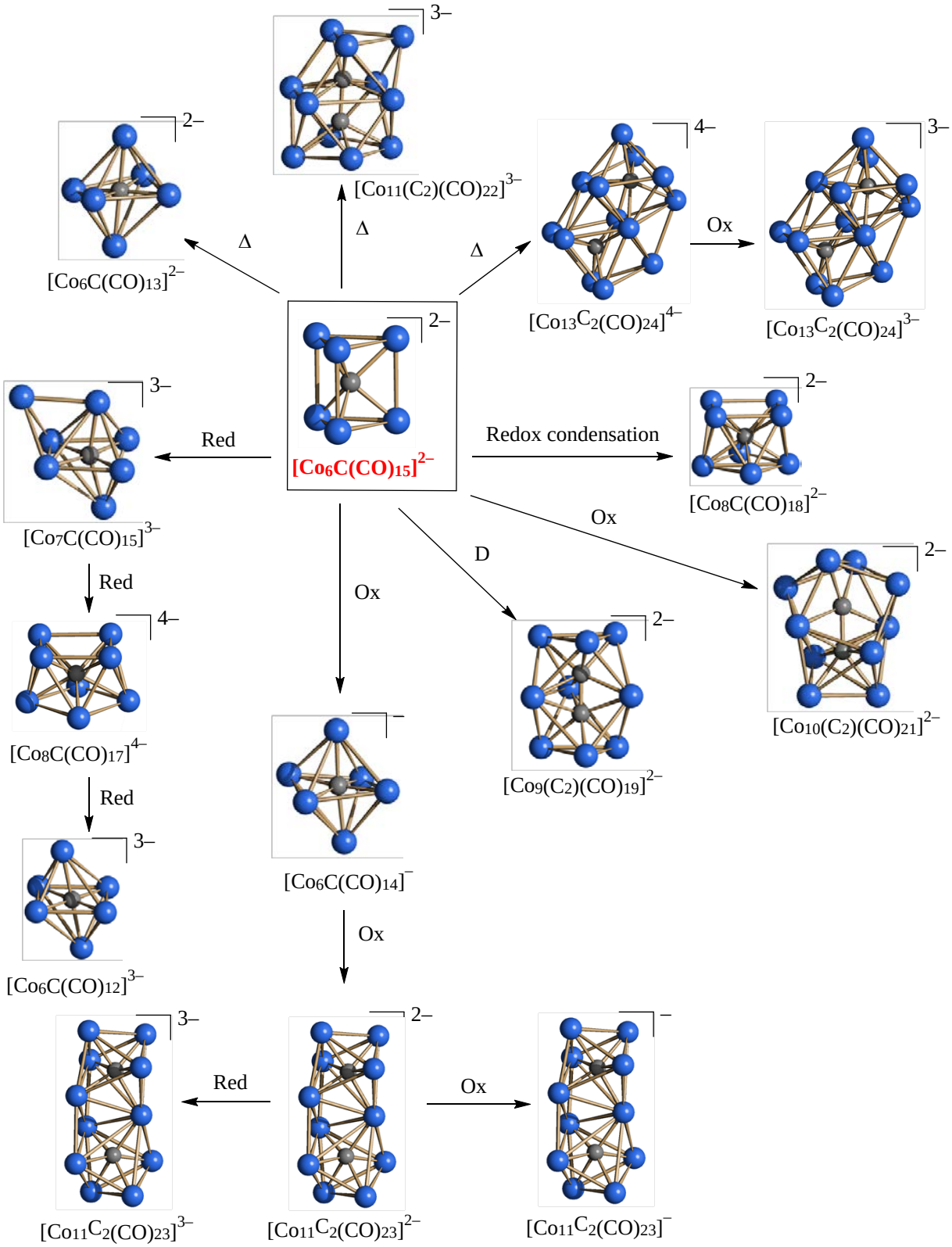

Scheme 4. Synthesis of Co carbide carbonyl clusters (Ox = oxidation; Red = reduction; Δ = thermal reaction). Several homometallic Co carbide carbonyl clusters are prepared by thermal or redox reactions starting from $[Co_6C(CO)_{15}]^{2-}$. See text and ref. [11] for details. CO ligands have been omitted for clarity (blue, Co; grey, C).

From a structural point of view, Co carbonyl mono-carbides may include the C-atom within: (a) a trigonal prismatic (TP) cage, *i.e.*, $[Co_6C(CO)_{15}]^{2-}$; (b) an octahedral (Oh) cage, *i.e.* $[Co_6C(CO)_{14}]^{-}$, $[Co_6C(CO)_{13}]^{2-}$, $[Co_6C(CO)_{12}]^{3-}$, $[Co_7C(CO)_{15}]^{3-}$; (c) a square-antiprismatic (SA) cage, *i.e.* $[Co_8C(CO)_{18}]^{2-}$ and $[Co_8C(CO)_{17}]^{4-}$ (Figure 3). All these species are diamagnetic, except $[Co_6C(CO)_{14}]^{-}$ and $[Co_6C(CO)_{12}]^{3-}$, which are paramagnetic as demonstrated by EPR measurements (Figure 4).

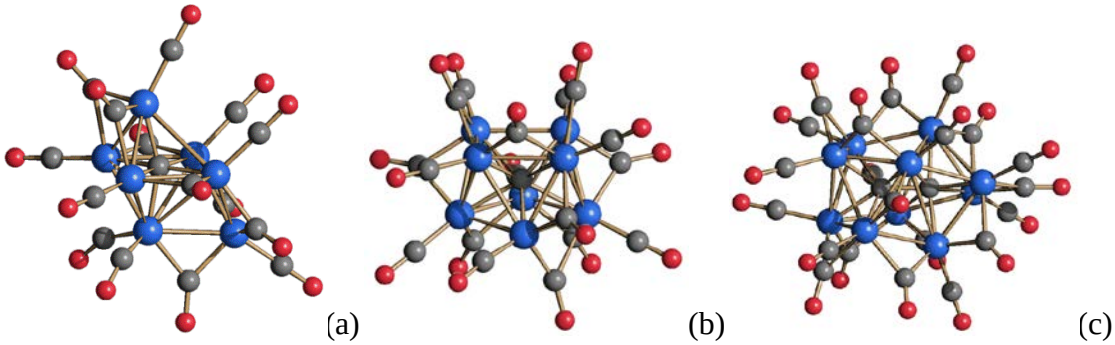

Fig. 3. Molecular structures of the mono-carbides (a) $[Co_7C(CO)_{15}]^{3-}$ and (b) $[Co_8C(CO)_{17}]^{4-}$, and the mono-acetylide (c) $[Co_{10}(C_2)(CO)_{21}]^{2-}$ (blue, Co; red, O; grey, C).

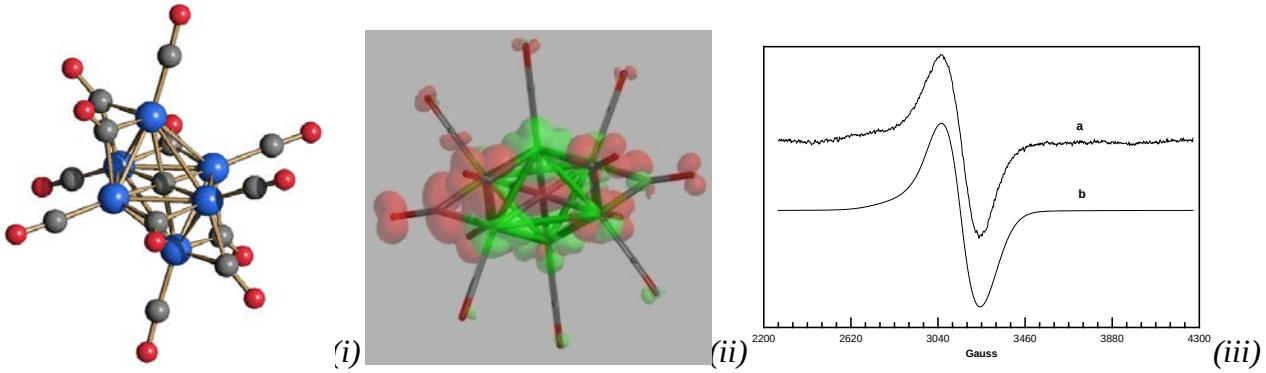

Fig. 4. (i) Molecular structure of $[Co_6C(CO)_{12}]^{3-}$ (blue, Co; red, O; grey, C); (ii) DFT calculated spin density surface (0.002 electron/au^3) of the $[Co_6C(CO)_{12}]^{3-}$ cluster (red, negative spin density; green, positive spin density); (iii) X band EPR spectrum of $[NMe_3(CH_2Ph)]_3[Co_6C(CO)_{12}]\cdot 4MeCN$ in MeCN solution registered at 203 K: (a) experimental and (b) simulation. Reproduced with permission from ref. 78.

The di-carbides $[Co_{11}C_2(CO)_{23}]^{n-}$ (n = 1-3) and $[Co_{13}C_2(CO)_{24}]^{n-}$ (n = 3,4) results from the condensation of two octahedral and two trigonal prismatic cages, respectively. Due to the stabilizing effect of the interstitial isolated C-atoms, both these species display reversible chemical and electrochemical redox processes. Moreover, it has been possible to isolate and structurally characterize differently charged anions, that is, $[Co_{11}C_2(CO)_{23}]^{n-}$ (n = 1,2) and $[Co_{13}C_2(CO)_{24}]^{n-}$ (n = 3,4) (Figure 5) [78,81]. In addition, both $[Co_{11}C_2(CO)_{23}]^{2-}$ and $[Co_{13}C_2(CO)_{24}]^{4-}$ demonstrated to be very active as

electrocatalysts for the hydrogen evolution reaction (HER) [54,55]. Indeed, the many metal-metal bonds in such clusters statistically enhance proton transfer (PT) rates and considerably increase the turnover frequency (TOF).

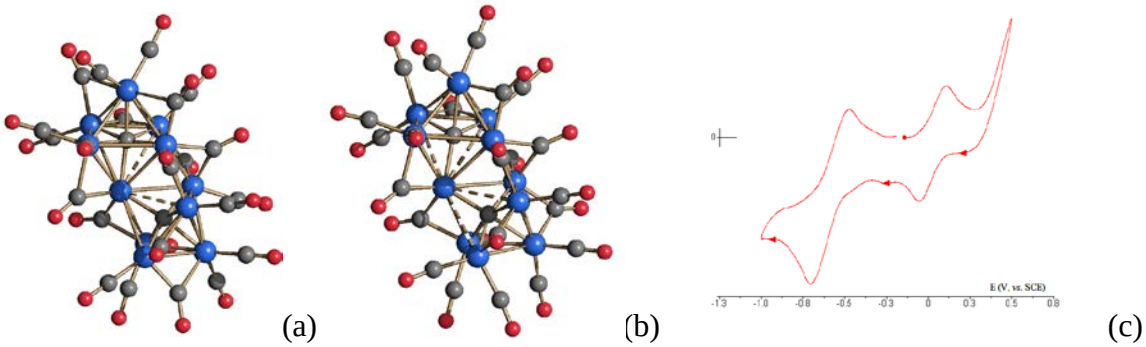

Fig. 5. Molecular structures of (a) $[Co_{11}C_2(CO)_{23}]^-$ and (b) $[Co_{11}C_2(CO)_{23}]^{2-}$ (blue, Co; red, O; grey, C). Co-Co contacts ≤ 3.02 Å are represented as full lines, those in the range 3.02-3.35 Å as fragmented lines. (c) Cyclic voltammogram recorded at a gold electrode in THF of $[NMe_3(CH_2Ph)]_2[Co_{11}C_2(CO)_{23}]$ (2.0×10^{-3} M). $[NBu_4][BF_4]$ (0.1 M) supporting electrolyte. Scan rate 0.1 Vs^{-1}. Reproduced with permission from ref. 78.

Larger cages are present in mono-acetylide species, *i.e.*, $[Co_9(C_2)(CO)_{19}]^{2-}$, $[Co_{10}(C_2)(CO)_{21}]^{2-}$ and $[Co_{11}(C_2)(CO)_{22}]^{3-}$, in order to accommodate a tightly bonded C_2 unit. Indeed, the C-C contacts are rather short indicating strong direct bonds, that is, 1.386 Å $[Co_9(C_2)(CO)_{19}]^{2-}$, 1.506 Å $[Co_{10}(C_2)(CO)_{21}]^{2-}$ and 1.527 Å $[Co_{11}(C_2)(CO)_{22}]^{3-}$. For comparison, typical distances for C-C single, double and triple bonds in organic molecules are 1.53, 1.34 and 1.14 Å.

4.2 Heterometallic Cobalt Carbide Carbonyl Clusters

Heterometallic Co-based carbide carbonyl clusters may be prepared following three general synthetic procedures:

1) Reaction of $Co_3(\mu_3\text{-}CCl)(CO)_9$ with metal carbonyl complexes or clusters;

2) Redox condensation involving a Co carbide carbonyl cluster and a metal complex, salt or cluster;

3) Addition of cationic metal fragments to an anionic Co carbide carbonyl cluster with the formation of a Lewis-type acid–base adduct.

4.2.1 Reaction of $Co_3(\mu_3\text{-}CCl)(CO)_9$ with metal carbonyl complexes or clusters

Synthesis (1) is well exemplified in the preparation of Co-Ni heterometallic carbide clusters [83-85]. Thus, addition of $Co_3(\mu_3\text{-}CCl)(CO)_9$ to $[Ni_6(CO)_{12}]^{2-}$ results in $[Co_3Ni_9C(CO)_{20}]^{3-}$, whereas

$[Co_6Ni_2C_2(CO)_{16}]^{2-}$ is obtained reversing the order of the reagents, that is, adding $[Ni_6(CO)_{12}]^{2-}$ to $Co_3(\mu_3\text{-}CCl)(CO)_9$. The mono-acetylide $[Co_3Ni_7(C_2)(CO)_{15}]^{3-}$ is formed via C-C coupling and redox condensation of $Co_3(\mu_3\text{-}CCl)(CO)_9$ with $[Ni_9C(CO)_{17}]^{2-}$. The redox condensation of $[Ni_{10}(C_2)(CO)_{16}]^{2-}$ and $Co_3(\mu_3\text{-}CCl)(CO)_9$ (Scheme 5) affords the Co–Ni hexa-carbide carbonyl nanocluster $[H_{6-n}Ni_{22}Co_6C_6(CO)_{36}]^{n-}$ (n = 3–6) [86], which can be thermally converted into the larger octa-carbide $[Ni_{36}Co_8C_8(CO)_{48}]^{6-}$ [87].

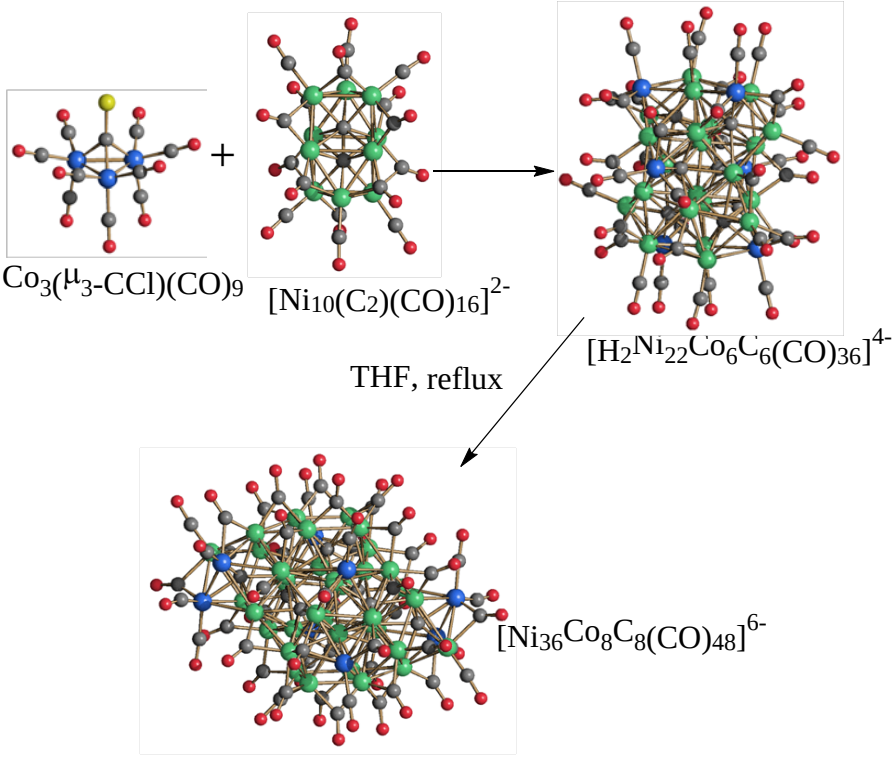

Scheme 5. Synthesis of $[H_2Ni_{22}Co_6C_6(CO)_{36}]^{4-}$ and $[Ni_{36}Co_8C_8(CO)_{48}]^{6-}$ (green, Ni; blue, Co; yellow, Cl; red, O; grey, C). Redox condensation of $[Ni_{10}(C_2)(CO)_{16}]^{2-}$ and $Co_3(\mu_3\text{-}CCl)(CO)_9$ affords $[H_2Ni_{22}Co_6C_6(CO)_{36}]^{4-}$, which is thermally converted into $[Ni_{36}Co_8C_8(CO)_{48}]^{6-}$. Reproduced with permission from ref. 11.

As systematically observed for large MCCs, the UV-visible spectra of $[H_{6-n}Ni_{22}Co_6C_6(CO)_{36}]^{n-}$ (n = 3–6) and $[H_{6-n}Ni_{36}Co_8C_8(CO)_{48}]^{n-}$ (n = 4-6) are featureless and almost identical (Figure 6). More interestingly, such species undergo a rich series of reversible protonation/deprotonation reactions as the result of the addition of stoichiometric amounts of strong acids such as $HBF_4{\cdot}Et_2O$, and bases such as NaOH. This phenomenon is quite common for high nuclearity MCCs. Such protonation/deprotonation reactions result in the stepwise decrease/increase of one unit of the anionic charge of the clusters, as clearly indicated by IR spectroscopy. Indeed, more charged anionic clusters show ν_{CO} bands at lower wave-numbers compared to less charged ones. Unfortunately, all attempts to directly confirm the

presence and number of hydride ligands in large MCCs by ^{1}H NMR spectroscopy failed independently of the experimental conditions (temperature, solvent, scan delay, field, solution or solid-state NMR). As it will be discussed in detail in Sections 4.2.2 and 5.3, it seems that above a nuclearity of *ca*. 20-30 metal atoms, molecular MCCs become NMR silent as indicated by the complete absence of any ^{1}H resonance in the hydride region [88].

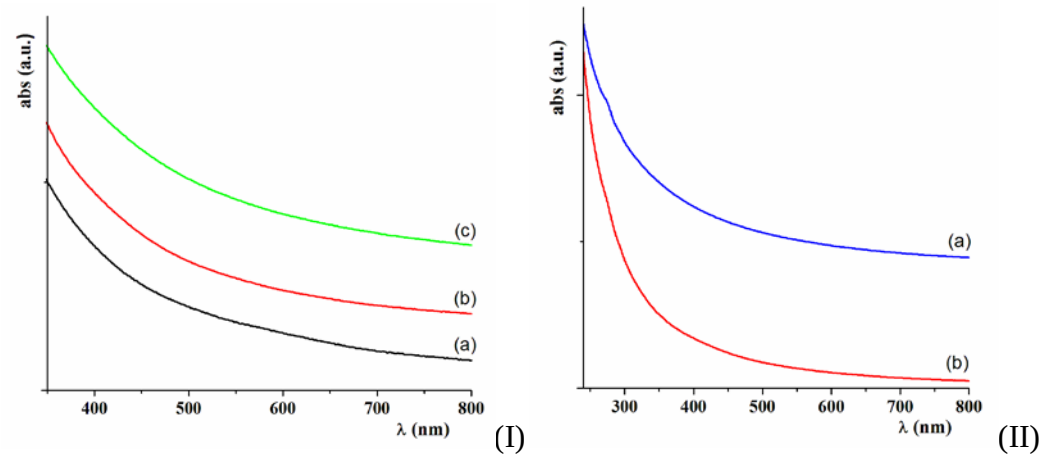

Fig. 6. (I) Normalised UV-visible spectra of (a) $[Ni_{36}Co_8C_8(CO)_{48}]^{6-}$ (10^{-5} M in MeCN); (b) $[HNi_{36}Co_8C_8(CO)_{48}]^{5-}$ (10^{-5} M in MeCN); (c) $[H_2Ni_{36}Co_8C_8(CO)_{48}]^{4-}$ (10^{-5} M in acetone). (II) Normalised UV-visible spectra in MeCN solution (10^{-5} M) of (a) $[HNi_{22}Co_6C_6(CO)_{36}]^{5-}$ and (b) $[HNi_{36}Co_8C_8(CO)_{48}]^{5-}$. Reproduced with permission from ref. 87.

4.2.2 Redox condensation of Cobalt Carbide Carbonyl Clusters

Redox condensation (synthesis 2) has been successfully employed for the preparation of heterometallic Co-Pt and Co-Pd poly-carbide carbonyl clusters. The reactions of $[Co_6C(CO)_{15}]^{2-}$ with $Pt(Et_2S)_2Cl_2$ and $Pd(Et_2S)_2Cl_2$ afford $[Co_8Pt_4C_2(CO)_{24}]^{2-}$ and $[H_2Co_{20}Pd_{16}C_4(CO)_{48}]^{4-}$, respectively [89,90]. Both these species revealed very interesting chemical, structural and physical properties.

The molecular structure of $[Co_8Pt_4C_2(CO)_{24}]^{2-}$ is composed of three face-sharing octahedra, the external ones being centered by the carbide atoms [89]. The two Pt atoms are disordered over the six positions of the internal octahedron. The $^{13}C\{^{1}H\}$ NMR spectrum on a $^{13}C_{carbide}$ enriched sample shows the presence of a non-polynomial quintet at δ_C 353.9 ppm ($^{1}J_{Pt\text{-}C}$ = 396 Hz) indicating the equivalence of the two carbides. In the cyclic voltammetric time scale, $[Co_8Pt_4C_2(CO)_{24}]^{2-}$ displays two reduction processes (E°' = –0.91 and –1.38 V vs. SCE) and one oxidation (E°' = +0.18 V) all possessing features of electrochemical reversibility (Figure 7). Thus, the complete series of $[Co_8Pt_4C_2(CO)_{24}]^{n-}$ (n = 1-4) clusters has been electrochemically characterized and, in addition, the mono-anion $[Co_8Pt_4C_2(CO)_{24}]^{-}$ has been also obtained by chemical oxidation of the di-anion and structurally characterized by SC-XRD, showing to be isostructural with $[Co_8Pt_4C_2(CO)_{24}]^{2-}$. Conversely, the more reduced species in the series

(n = 3 and 4) are not stable enough to be isolated. Indeed, the chemical reduction of $[Co_8Pt_4C_2(CO)_{24}]^{2-}$ with Na/naphthalene resulted, after work-up of the reaction mixtures, in the isolation of $[Co_{10}Pt_2C_2(CO)_{22}]^{4-}$ and $[Co_8Pt_4C_2(CO)_{20}]^{4-}$ [91].

As expected, the odd-electron mono-anion $[Co_8Pt_4C_2(CO)_{24}]^{-}$ is paramagnetic because of the presence of one unpaired electron in the SOMO, resulting in a doublet state (S = 1/2). More interestingly, solid state EPR and SQUID measurements at variable temperature indicate that also the even-electron di-anion $[Co_8Pt_4C_2(CO)_{24}]^{2-}$ is paramagnetic, due to a S = 1 triplet state (Figure 8). The magnetic behavior of even-electron MCCs has been debated for very longtime [92], and the studies on $[Co_8Pt_4C_2(CO)_{24}]^{2-}$ clearly indicate that genuine cases of paramagnetism in even-electron MCCs are possible.

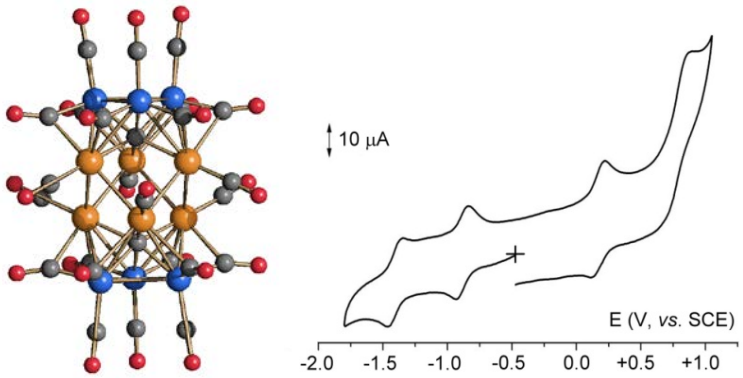

Fig. 7. (a) Molecular structure of $[Co_8Pt_4C_2(CO)_{24}]^{n-}$ (n = 1,2). Co as blue sphere, disordered Co/Pt orange, C gray and O red. (b) Cyclic voltammetric response recorded at a glassy carbon electrode in THF solution of crystalline $[NMe_3(CH_2Ph)]_2[Co_8Pt_4C_2(CO)_{24}]$ (1.2×10^{-3} M). $[NBu_4][PF_6]$ (0.2 M) supporting electrolyte. Scan rates 0.2 V s^{-1}. Reproduced with permission from ref. 89.

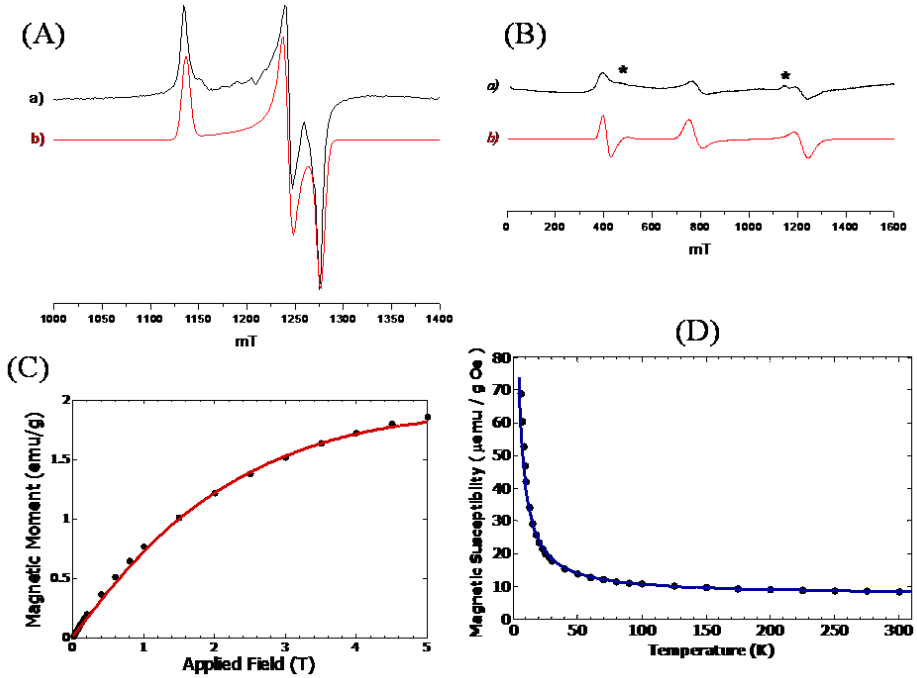

Fig. 8. EPR spectra in solid at 5 K of $[Co_8Pt_4C_2(CO)_{24}]^{n-}$: (a) n = 1, S = ½; (b) n = 2, S = 1 (* background impurity) Experimental spectra in black, simulated spectra in red. (c) First magnetization curve at 2 K and (d) temperature dependence of magnetization of $[Co_8Pt_4C_2(CO)_{24}]^{2-}$. Reproduced with permission from ref. 89.

The Co-Pd tetra-anion $[H_2Co_{20}Pd_{16}C_4(CO)_{48}]^{4-}$ (Scheme 6) is reversibly converted into the related $[H_{6-n}Co_{20}Pd_{16}C_4(CO)_{48}]^{n-}$ (n = 3-6) species after the addition of acids and bases [90]. The poly-hydride nature of these species has been supported by electrochemical studies. The isostructural tetra-anion $[H_2Co_{20}Pd_{16}C_4(CO)_{48}]^{4-}$ and the penta-anion $[HCo_{20}Pd_{16}C_4(CO)_{48}]^{5-}$ have been characterized by SC-XRD. They are both based on a cubic close-packed (ccp) Pd_{16} core decorated on its surface by four square-pyramidal $\{Co_5C(CO)_{12}\}$ organometallic fragments.

Further addition of acids after the formation of the tri-anion $[H_3Co_{20}Pd_{16}C_4(CO)_{48}]^{3-}$ results in $[H_{3-n}Co_{15}Pd_9C_3(CO)_{38}]^{n-}$ (n = 0–3) [93], with formal degradation of the ccp Pd_{16} core to Pd_9. By employing a larger excess of acid, $[Co_{13}Pd_3C_3(CO)_{29}]^{-}$, which contains a Pd_3, core is eventually formed [94].

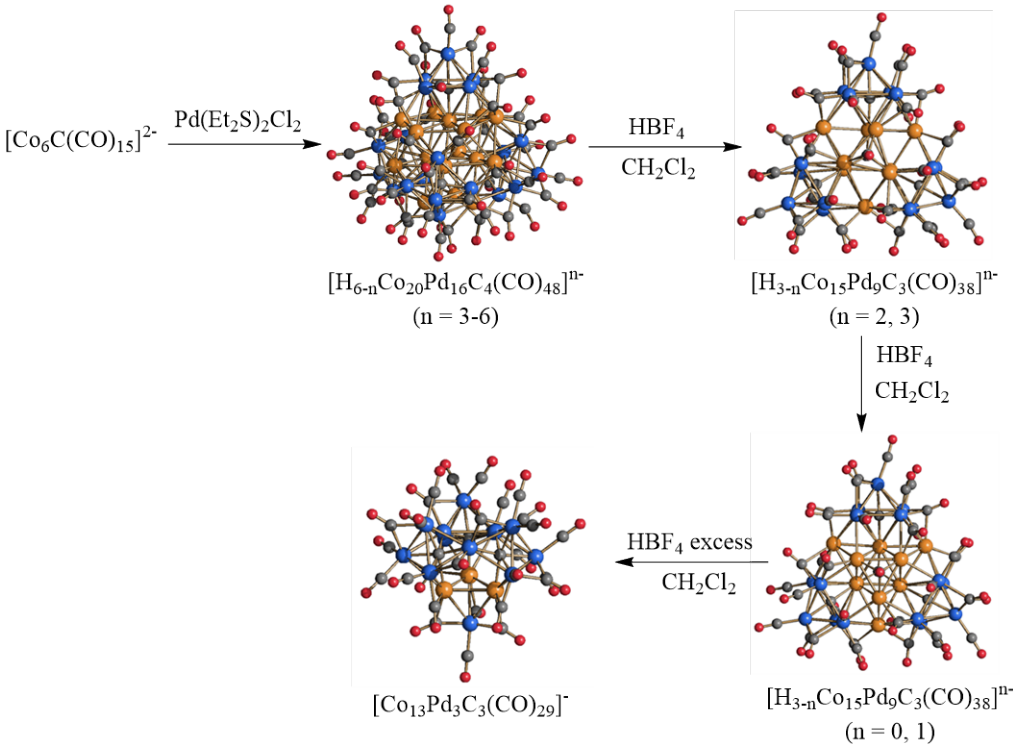

Scheme 6. Synthesis and reactivity of $[H_{6-n}Co_{20}Pd_{16}C_4(CO)_{48}]^{n-}$ (n = 3–6) (orange, Pd; blue, Co; red, O, grey, C). This compound is obtained from the redox condensation of $[Co_6C(CO)_{15}]^{2-}$ and $Pd(Et_2S)_2Cl_2$. $[H_{6-n}Co_{20}Pd_{16}C_4(CO)_{48}]^{n-}$ (n = 3–6) is transformed into $[H_{3-n}Co_{15}Pd_9C_3(CO)_{38}]^{n-}$ (n = 0–3) and, eventually, $[Co_{13}Pd_3C_3(CO)_{29}]^-$ upon reaction with increasing amounts of strong acids. Reproduced with permission from ref. 11.

The species $[H_{3-n}Co_{15}Pd_9C_3(CO)_{38}]^{n-}$ (n = 0–3) can be inter-converted by reactions with acids and bases [93]. The neutral cluster $[H_3Co_{15}Pd_9C_3(CO)_{38}]$ is stable only in the solid state, whereas it is immediately deprotonated to the mono-anion $[H_2Co_{15}Pd_9C_3(CO)_{38}]^-$ after dissolution in CH_2Cl_2. The cyclic voltammetries of the three anions $[H_{3-n}Co_{15}Pd_9C_3(CO)_{38}]^{n-}$ (n = 1–3) revealed that they are multivalent since they undergo two or three chemically reversible oxidations (Figure 9). The different electrochemical behaviours of these three cluster anions further support the fact that they are different chemical species and not the same cluster with a different charge. In particular, the fact that they display only oxidation processes rules out the possibility that a less charged species might be transformed into a more charged one by a redox reaction. Indeed, this should be a reduction, which is not observed in their electrochemistry. Therefore, the transformation of a less charged cluster into a more charged one can be achieved only by removal of a proton by means of an acid/base reaction. All these considerations suggest the formulation of these clusters as poly-hydrides. Moreover, the chemical and electrochemical behaviour of $[H_{3-n}Co_{15}Pd_9C_3(CO)_{38}]^{n-}$ (n = 0–3) clearly point out that their charges can be changed both

by acid-base and redox reactions, even if differently. This is a common behaviour often found in large MCCs, which makes their study complicated but fascinating.

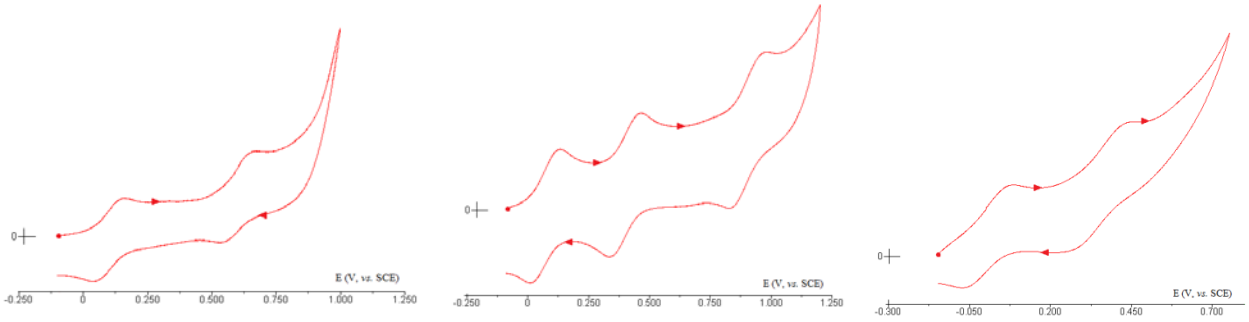

(a) (b) (c)

n	3–/2–	2–/1–	1–/0	0/+1
1	-	-	+0.104	+0.600
2	-	+0.067	+0.398	+0.899
3	+0.002	+0.347	-	-

Fig. 9. Cyclic voltammograms recorded at a glassy carbon electrode in CH_2Cl_2 of (a) $[H_2Co_{15}Pd_9C_3(CO)_{38}]^-$, (b) $[HCo_{15}Pd_9C_3(CO)_{38}]^{2-}$ and (c) $[Co_{15}Pd_9C_3(CO)_{38}]^{3-}$ (2.0×10^{-3} M). $[NBu_4][BF_4]$ (0.1 M) supporting electrolyte. Scan rate 0.2 Vs^{-1}. The table reports the formal electrode potentials (in V, vs. S.C.E.) for the redox changes exhibited by $[H_{3-n}Co_{15}Pd_9C_3(CO)_{38}]^{n-}$ (n = 1–3). Solvent discharge occurs at high potentials. Reproduced with permission from ref. 93.

SQUID measurements on a crystalline sample of $[NMe_3(CH_2Ph)]_2[HCo_{15}Pd_9C_3(CO)_{38}]\cdot C_6H_{14}$ indicates its paramagnetism due to two unpaired electrons (S=1) [93]. This gives further support to its formulation as an even-electron mono-hydride. Moreover, as observed for $[Co_8Pt_4C_2(CO)_{24}]^{2-}$, these findings clearly indicate that even-electron MCCs of increasing sizes can be paramagnetic.

The molecular structures of the four species $[H_{3-n}Co_{15}Pd_9C_3(CO)_{38}]^{n-}$ (n = 0–3) have been determined by SC-XRD on miscellaneous salts [93,94]. They are composed of a $Pd_9(\mu_3\text{-}CO)_2$ core decorated by three square-pyramidal $\{Co_5C(CO)_{12}\}$ organometallic fragments. The Pd_9 kernel adopts a tricapped octahedral structure (Oh-Pd_9) in the less charged species, that is, $[H_3Co_{15}Pd_9C_3(CO)_{38}]$ and $[H_2Co_{15}Pd_9C_3(CO)_{38}]^-$, whereas it becomes a tricapped trigonal prism (TP-Pd_9) in the tri-anion $[Co_{15}Pd_9C_3(CO)_{38}]^{3-}$. Interestingly, depending on the cations and/or co-crystallization solvent, the di-anion $[HCo_{15}Pd_9C_3(CO)_{38}]^{2-}$ may adopt in the solid state both the Oh-Pd_9 and TP-Pd_9 structure [94]. Moreover, in some cases both the Oh-Pd_9 and TP-Pd_9 isomers have been found in the same crystallization batch, as mixtures of different crystals or within the same crystal. This represent a rare case of cluster core isomerism in a large MCC [95,96]. Generally speaking, it seems that, first of all,

there is an effect on the Oh/TP structure related to the charge (number of hydrides) of the cluster. Thus, the Oh-Pd_9 / TP-Pd_9 transformation may be induced by deprotonation/deprotonation reactions (Figure 10). Then, in the case of the di-anion mono-hydride, it is likely that both isomers co-exist (or rapidly inter-convert) in solution and, depending on the crystallization conditions, one or the other (or a mixture of the two) isomers precipitate out of the solution.

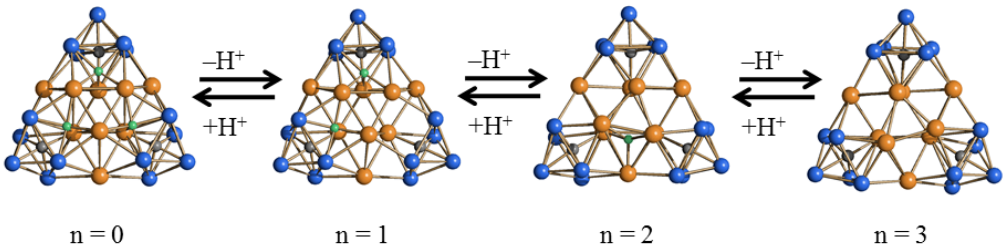

Fig. 10. Protonation-deprotonation induced structural rearrangement of the $[H_{3-n}Co_{15}Pd_9C_3(CO)_{38}]^{n-}$ (n = 0-3) clusters. Reproduced with permission from ref. 93.

4.2.3 Addition of Lewis Acids to Cobalt Carbide Carbonyl Clusters

The reactions of $[Co_6C(CO)_{15}]^{2-}$ with $Au(PPh_3)Cl$ may result in different products, depending on the experimental conditions (Scheme 7) [97-99]. All the products may be viewed as adducts between cobalt carbide carbonyl anions such as $[Co_6C(CO)_{12}]^{4-}$, $[Co_5C(CO)_{12}]^{-}$, $[Co_5C(CO)_{11}]^{3-}$, and $[Co_4C(CO)_{10}]^{2-}$, which act as Lewis bases, and the Lewis acid $[Au(PPh_3)]^{+}$. It must be remarked that the homometallic anions just listed are not known as free species. Some of these Co-Au clusters can exist as different isomers in the solid state. For instance, three different isomers have been structurally characterized in the case of $[Co_6C(CO)_{12}(AuPPh_3)_4]$ (Figure 11). All of them have been crystallized by slow diffusion of n-hexane into a THF solution of the cluster. The resulting solid may contain one or a mixture of the three isomers, which differ by the amount of co-crystallized solvent, that is, $[Co_6C(CO)_{12}(AuPPh_3)_4]$, $[Co_6C(CO)_{12}(AuPPh_3)_4]\cdot THF$ and $[Co_6C(CO)_{12}(AuPPh_3)_4]\cdot 4THF$. Computational studies by DFT methods indicate that formation of the different isomers upon crystallization results from a subtle balance among packing and van der Waals forces, as well as aurophilic and weak π-π and π-H interactions [99].

1) Amount of [Au(PPh$_3$)Cl]

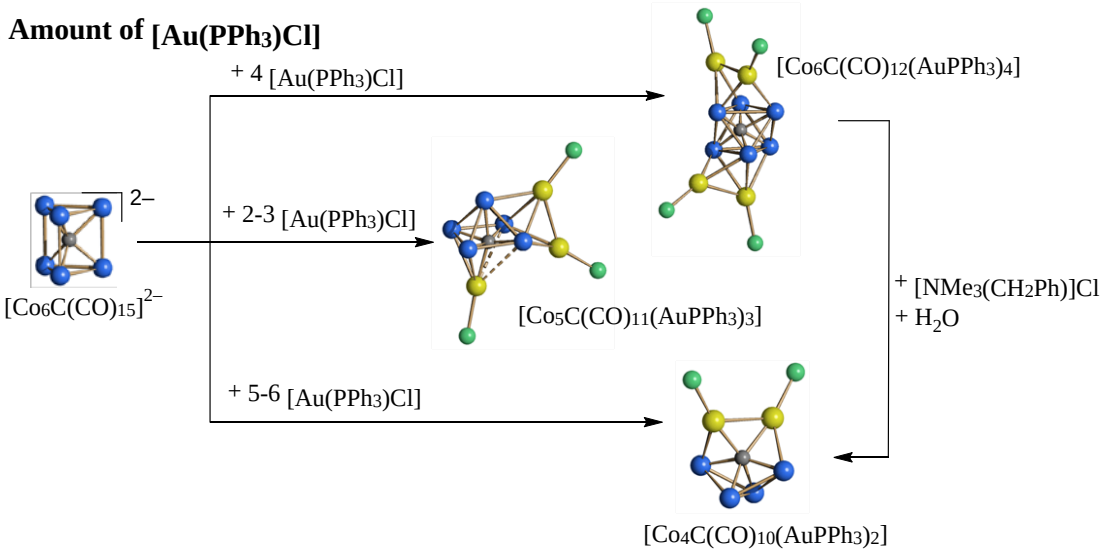

2) With free PPh$_3$

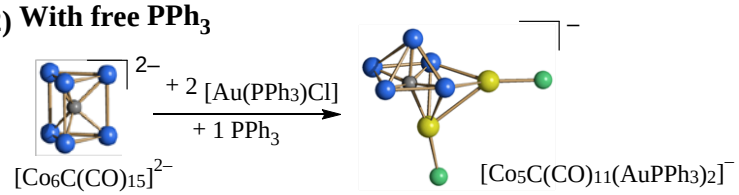

3) Silver salts

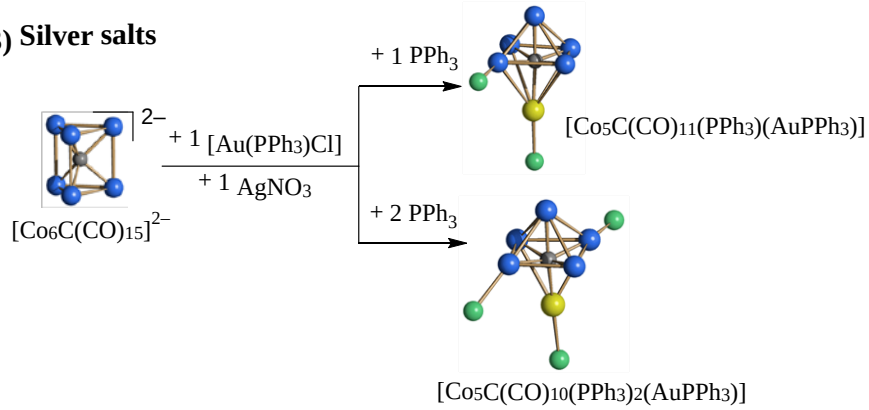

4) Other methods

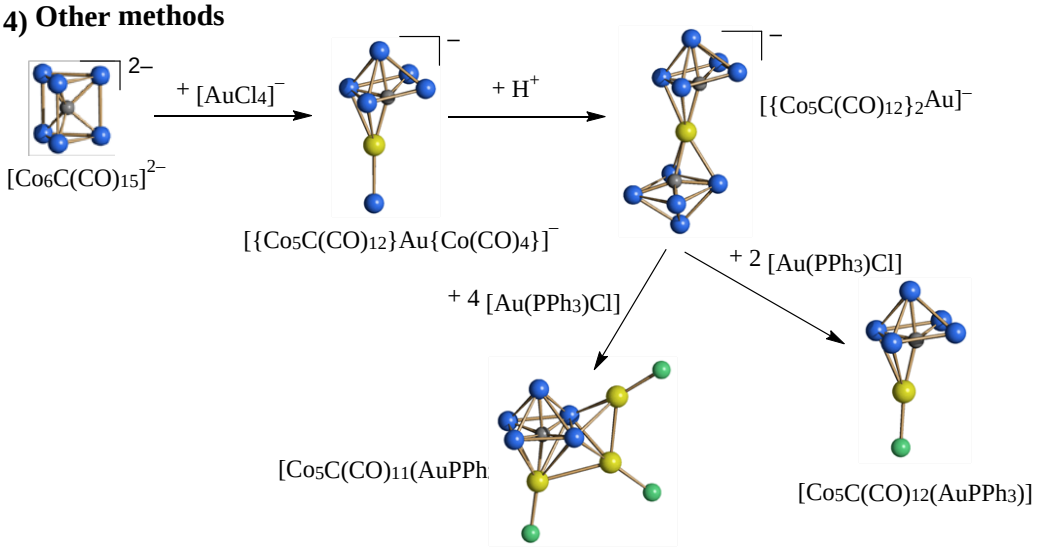

Scheme 7. Synthesis of Co-carbide carbonyl clusters decorated by $AuPPh_3$ fragments. CO ligands and Ph groups have been omitted for clarity (blue, Co; yellow, Au; green, P; grey, C).

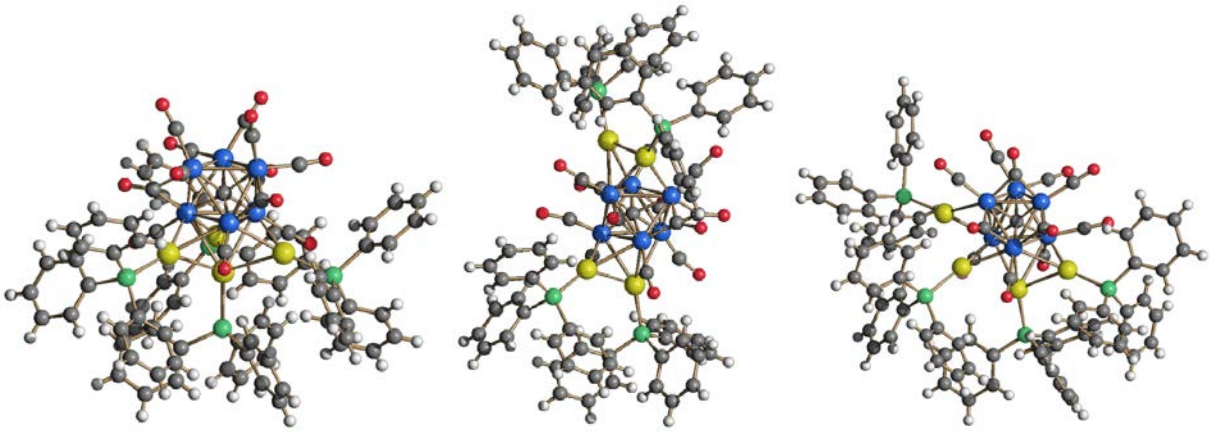

Fig. 11. The three isomers of $[Co_6C(CO)_{12}(AuPPh_3)_4]$ as found in the crystals of $[Co_6C(CO)_{12}(AuPPh_3)_4]$, $[Co_6C(CO)_{12}(AuPPh_3)_4]\cdot THF$ and $[Co_6C(CO)_{12}(AuPPh_3)_4]\cdot 4THF$ (blue, Co; yellow, Au; green, P; red, O; grey, C; white, H).

The homoleptic Co-Au carbide cluster $[\{Co_5C(CO)_{12}\}Au\{Co(CO)_4\}]^-$ is obtained from the reaction of $[Co_6C(CO)_{15}]^{2-}$ with two equivalents of $[AuCl_4]^-$, and it is converted into $[\{Co_5C(CO)_{12}\}_2Au]^-$ upon addition of strong acids [100]. Both $[\{Co_5C(CO)_{12}\}Au\{Co(CO)_4\}]^-$ and $[\{Co_5C(CO)_{12}\}_2Au]^-$ may be described as Au(I) complexes containing $[Co_5C(CO)_{12}]^-$ and $[Co(CO)_4]^-$ as ligands. These two clusters display several chemically reversible redox processes, and all the species $[\{Co_5C(CO)_{12}\}Au\{Co(CO)_4\}]^{n-}$ (n = 1-3) and $[\{Co_5C(CO)_{12}\}_2Au]^{n-}$ (n = 0-3) have been characterized by electrochemical and spectroelectrochemical methods (Figure 12). The redox processes are mainly centred on the $[Co_5C(CO)_{12}]^-$ fragments as demonstrated by DFT investigations. The limited stability of the reduced species hampers their chemical isolation, and it is likely due to an intra-molecular (inner sphere) redox reaction which lead to formation of Au(0) and cluster fragmentation.

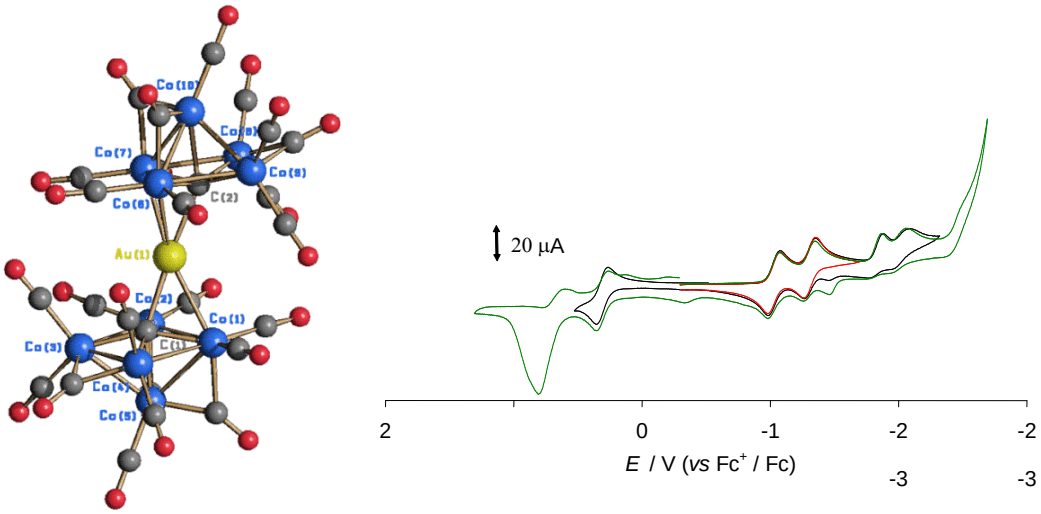

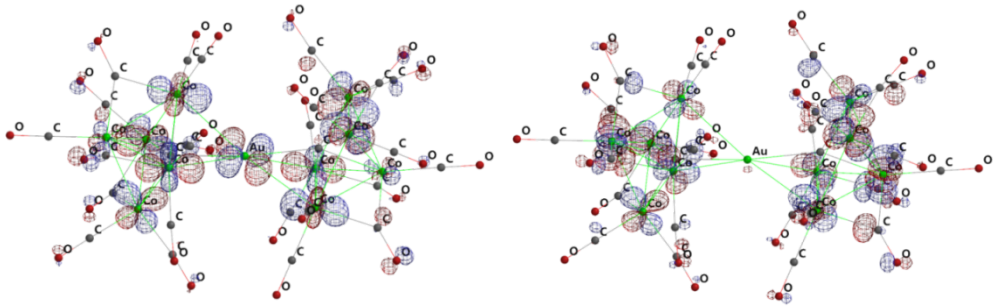

HOMO LUMO

Fig. 12. Molecular structure, cyclic voltammograms (recorded at a platinum electrode in a CH_2Cl_2 solution; $[N^nBu_4][PF_6]$ 0.2 mol dm^{-3} as supporting electrolyte; scan rate 0.1 V s^{-1}), HOMO and LUMO (DFT EDF2 calculations, isovalue = 0.04 a.u) of $[\{Co_5C(CO)_{12}\}_2Au]^-$. Reproduced with permission from ref. 100.

5. Nickel Carbide Carbonyl Clusters

5.1 Synthesis of Nickel Carbide Carbonyl Clusters

Nickel carbide carbonyl clusters represent the richest class of homometallic clusters containing interstitial carbide atoms [11,35,101-103]. These include clusters containing from 7 up to 45 Ni atoms and, the largest species may be viewed as atomically precise metal nanoclusters. Such clusters can include from one up to ten interstitial carbide atoms, as well as from one up to four C_2 acetylide units.

Several Ni carbide carbonyl clusters can be directly prepared from the reaction of $[Ni_6(CO)_{12}]^{2-}$ with carbon halides (*e.g.*, CCl_4, C_2Cl_4, C_2Cl_6, C_3Cl_6, C_4Cl_6). Different species are obtained depending on the carbon source, the stoichiometry of the reaction, the solvent and temperature (Scheme 8). For instance, the reaction of $[Ni_6(CO)_{12}]^{2-}$ with increasing amounts of CCl_4 in THF, acetone or MeCN results in $[Ni_{10}C(CO)_{18}]^{2-}$, $[Ni_9C(CO)_{17}]^{2-}$, and, eventually, $[Ni_8C(CO)_{16}]^{2-}$. Conversely, performing the same reaction in CH_2Cl_2 affords $[HNi_{25}(C_2)_4(CO)_{32}]^{3-}$ by employing a $CCl_4/[Ni_6(CO)_{12}]^{2-}$ ratio of 1.15, whereas $[Ni_{22}(C_2)_4(CO)_{28}Cl]^{3-}$ represents the major product when $CCl_4/[Ni_6(CO)_{12}]^{2-}$ = 1.43 [104,105]. Lower values of $CCl_4/[Ni_6(CO)_{12}]^{2-}$ (0.5-0.9) result in mixtures of $[Ni_9C(CO)_{17}]^{2-}$, $[HNi_{34}C_4(CO)_{38}]^{5-}$ and $[HNi_{38}C_6(CO)_{42}]^{5-}$.

The reaction of $[Ni_6(CO)_{12}]^{2-}$ with C_2Cl_6 affords the mono-acetylide cluster $[Ni_{10}(C_2)(CO)_{16}]^{2-}$ when performed in acetone, whereas the bis-acetylide $[Ni_{16}(C_2)_2(CO)_{23}]^{4-}$ is obtained using MeCN as solvent. Related $[Ni_{16+x}(C_2)_2(CO)_{23+x}]^{4-}$ (x = 0, 1) species, differing for the presence/absence of an additional Ni(CO) fragment, have been obtained from $[Ni_6(CO)_{12}]^{2-}$ and C_4Cl_6 in CH_2Cl_2 or THF [104].

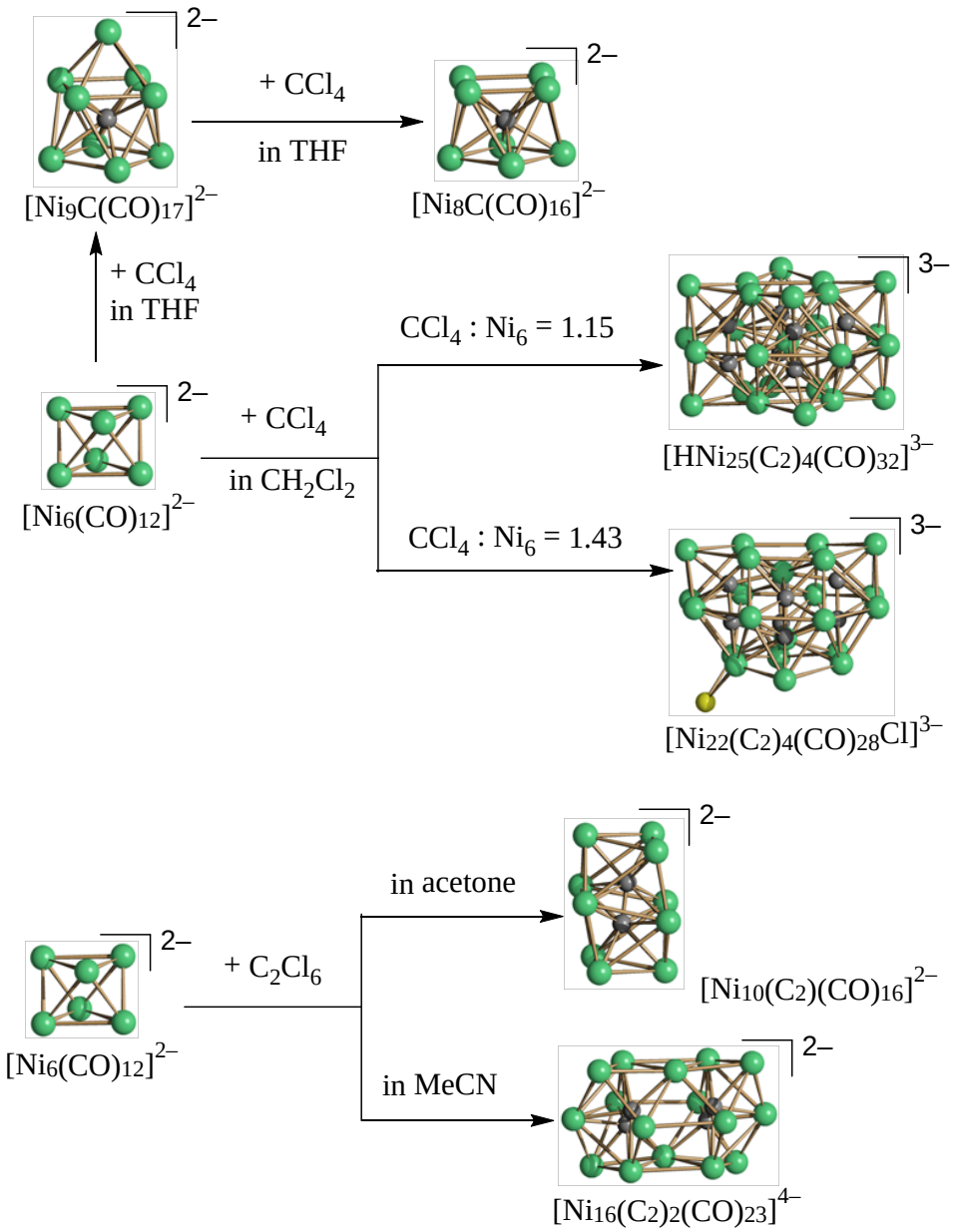

Scheme 8. Some direct syntheses of nickel carbide carbonyl clusters from $[Ni_6(CO)_{12}]^{2-}$ and carbon halides. CO ligands have been omitted for clarity (green, Ni; yellow, Cl; grey, C).

Preformed Ni carbide carbonyl clusters may be used for the preparation of further species by means of different reactions, such as oxidation, reduction, ligand induced rearrangement, redox condensation (Scheme 9). For instance, the reduction of $[Ni_9C(CO)_{17}]^{2-}$ with Na/naphthalene in THF affords $[Ni_{12}C(CO)_{18}]^{4-}$, whereas a mixture of $[Ni_{11}(C_2)(CO)_{15}]^{4-}$ and $[Ni_{12}(C_2)(CO)_{16}]^{4-}$ is obtained from $[Ni_{10}(C_2)(CO)_{16}]^{2-}$ and Na/naphthalene in THF [106]. Oxidation of $[Ni_{10}(C_2)(CO)_{16}]^{2-}$ with CuCl in THF results in the deca-carbide $[Ni_{45}C_{10}(CO)_{46}]^{6-}$ [35], whereas the tetra-acetylide $[Ni_{22}(C_2)_4(CO)_{28}(Et_2S)]^{2-}$ can be obtained from the reaction of $[Ni_{10}(C_2)(CO)_{16}]^{2-}$ with $Pd(Et_2S)_2Cl_2$ in THF (Figure 13) [106]. In both cases, the Cu(I) and Pd(II) salts acted as oxidants. More often, the

reactions of Ni carbide carbonyl anions with transition metal salts or complexes result in heterometallic carbide clusters via redox condensation or oxidation followed by addition of a positively charged metal fragment to the cluster surface. For instance, redox condensation is observed when $[Ni_9C(CO)_{17}]^{2-}$ is reacted with $[Rh(CODCl]_2$ resulting in a mixture of $[Ni_{10}Rh_2C(CO)_{20}]^{2-}$ and $[Ni_9Rh_3C(CO)_{20}]^{3-}$ [107].

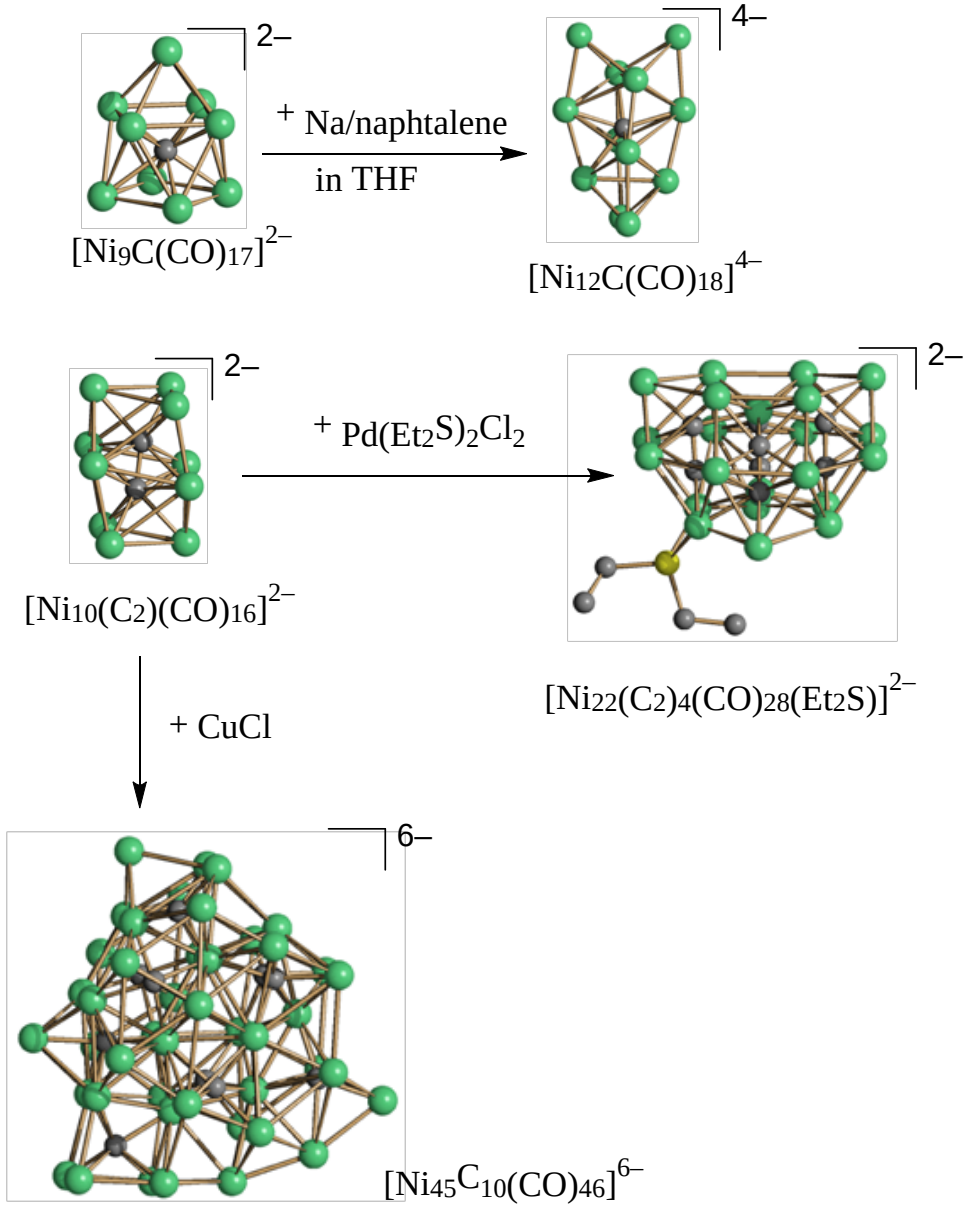

Scheme 9. Some representative syntheses of nickel carbide carbonyl clusters from preformed carbide clusters. CO ligands and H-atoms have been omitted for clarity (green, Ni; yellow, S; grey, C).

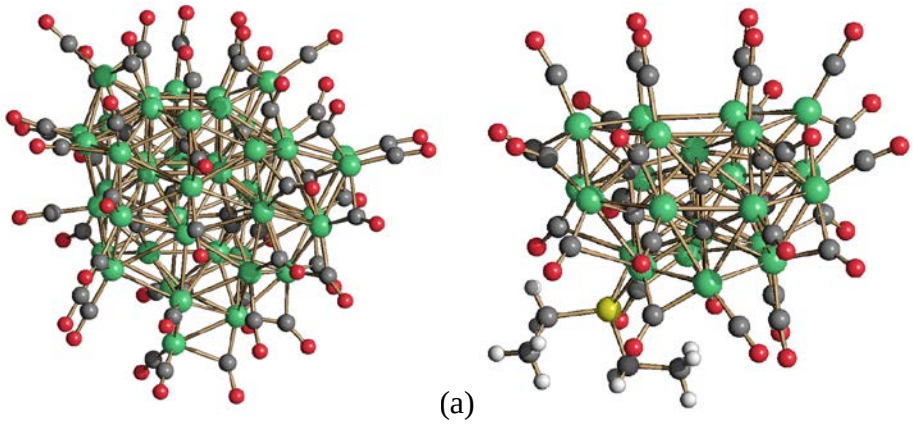

(a) (b)

Fig. 13. Molecular structure of (a) $[Ni_{45}C_{10}(CO)_{46}]^{6-}$ and (b) $[Ni_{22}(C_2)_4(CO)_{28}(Et_2S)]^{2-}$ (green, Ni; gray, C; red, O; yellow, S; white, H).

The reactions of $[Ni_9C(CO)_{17}]^{2-}$ and $[Ni_{10}(C_2)(CO)_{16}]^{2-}$ with Cd(II) and Cu(I) salts afford different Ni-Cd and Ni-Cu poly-carbide and poly-acetylide carbonyl clusters [35,88,103,108-111]. All these clusters may be described as composed of an anionic Ni-C-CO cage decorated by miscellaneous $[CdX]^+$, $[Cd_2Cl_3]^+$, $[Cu(MeCN)]^+$ and CuCl fragments. In these cases, Cd and Cu formally retain their original +2 and +1 oxidation state, and the clusters may be viewed as Lewis acid-base adducts (Figure 14). It is noteworthy that the inclusion of interstitial carbide atoms and the decoration of the surface with such cationic fragments lead to very large clusters that may be viewed as atomically precise metal nanoclusters.

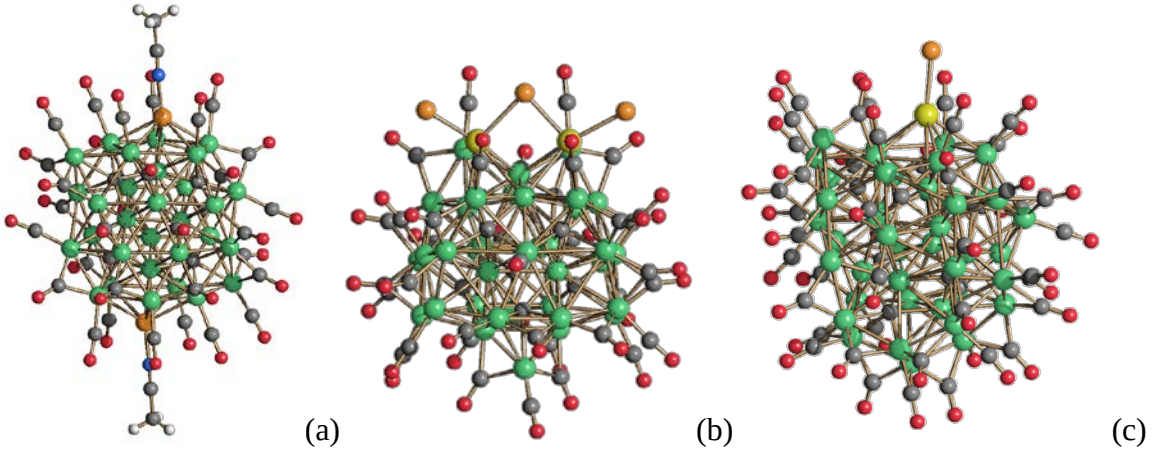

(a) (b) (c)

Fig. 14. Molecular structure of (a) $[H_2Ni_{30}C_4(CO)_{34}\{Cu(MeCN)\}_2]^{4-}$ (green, Ni; orange, Cu; grey, C; red, O; blue, N; white, H), (b) $[Ni_{36}C_8(CO)_{36}(Cd_2Cl_3)]^{5-}$ and (c) $[Ni_{42+x}C_8(CO)_{44+x}(CdCl)]^{7-}$ (x = 0.19) (green, Ni; yellow, Cd; orange, Cl; grey, C; red, O).

5.2 Structural features

Ni carbide carbonyl clusters may be divided into two main categories:

1) Carbide and poly-carbide clusters: these contain one or more isolated interstitial C atoms;

2) Acetylide and poly-acetylide clusters, containing one or more tightly bonded C_2 units.

So far, $[Ni_{12}(C)(C_2)(CO)_{17}(AuPPh_3)_3]^-$ is the only cluster structurally characterized that contains both a carbide and an acetylide unit (Figure 15) [112,113]. This species is rather interesting, since it displays weak van der Waals interactions between the C-atom and the C_2-unit [C(2)-C(3) 1.402(10) Å, C(1)···C(2) 2.781(11) Å; C(1)···C(3) 2.798(11) Å], suggesting the incipient formation of more extended C-C bonding within the metal cage of a molecular cluster. It is well known that Fe, Co and Ni nanoparticles catalyze the growth of carbon nanostructures, whose formation may likely depend on how C-fragments are stabilized and joined on a metal framework [114-117].

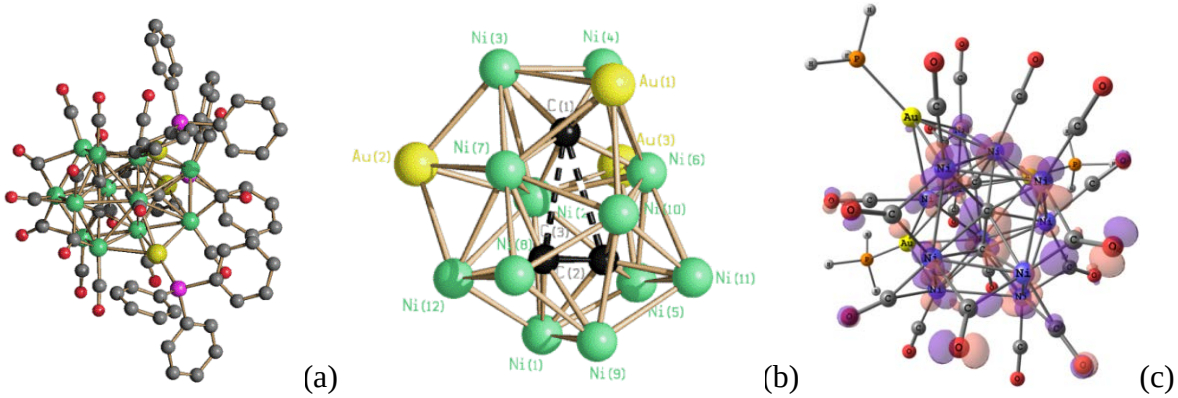

Fig. 15. (a) Molecular structure of $[Ni_{12}(C)(C_2)(CO)_{17}(AuPPh_3)_3]^-$ (green, Ni; yellow, Au; purple, P; red, O; grey, C; H-atoms have been omitted for clarity) and (b) its $Ni_{10}(C_2)$ fragment with the weak C···(C_2) interactions (fragmented lines). (c) HOMO of the model system $[Ni_{12}(C)(C_2)(CO)_{17}(AuPH_3)_3]^-$ (M06/6-31G(d,p)+LANL2TZ(f) calculations, surface isovalue = 0.05 a.u.) showing the π-bonding interaction between the carbon atoms of the acetylide unit. Reproduced with permission from ref. 112.

5.2.1 Nickel Carbide Carbonyl Clusters containing isolated C atoms

Ni carbide and poly-carbide carbonyl clusters are constituted of four main building units [35]: 1) octahedral Oh-Ni_6C cages; 2) trigonal prismatic TP-Ni_6C cages; 3) capped trigonal prismatic cTP-Ni_7C cages; 4) square anti-prismatic SA-Ni_8C cages. All these cages have been found isolated in mono-carbide clusters, or combined in poly-carbide clusters. The latter species may contain just one type of cage as well as two or three different types. Thus, Oh-Ni_6C, TP-Ni_6C, cTP-Ni_7C and SA-Ni_8C may be viewed as the fundamental building-blocks of all Ni carbide clusters reported so far. It is noteworthy that the Ni-Ni and the Ni-C distances within a single type of carbide cage are almost identical in all the clusters. This indicates that these building-blocks are quite rigid and their structures are not significantly altered after being joined into larger Ni_xC_y metal-carbide frameworks. These may result from sharing vertices, edges or faces between two or more Oh-Ni_6C, TP-Ni_6C, cTP-Ni_7C and SA-Ni_8C cages. These

Ni_xC_y frameworks may be further decorated on the surface by Ni atoms or other metals not directly connected to the carbides. As a consequence of these surface decoration motives, often the crystal structures of large Ni carbide carbonyl clusters display some composition disorder. This is indicated by the fractionary indices of their formulas. As an example, the crystals of $[NMe_4]_7[HNi_{42+2x}C_8(CO)_{44+2x}(CuCl)_{1-x}]\cdot 6.5MeCN$ (x = 0.14) contain a mixture of $[HNi_{42}C_8(CO)_{44}(CuCl)]^{7-}$ (86%) and $[HNi_{43}C_8(CO)_{45}]^{7-}/[HNi_{44}C_8(CO)_{46}]^{7-}$ (14%) (Figure 16) [103]. Similarly, $[NMe_4]_6[H_2Ni_{43+x}C_8(CO)_{45+x}]\cdot 6MeCN$ (x = 0.72) is a mixture of $[H_2Ni_{44}C_8(CO)_{46}]^{6-}$ (72%) and $[H_2Ni_{43}C_8(CO)_{45}]^{6-}$ (28%). Compositionally disordered clusters are at the border between molecular and quasi-molecular nanoclusters [108]. Alternatively, such disorder may be viewed as an incipient polydispersity of such molecular nanoclusters, which can be determined with atomic precision through SC-XRD.

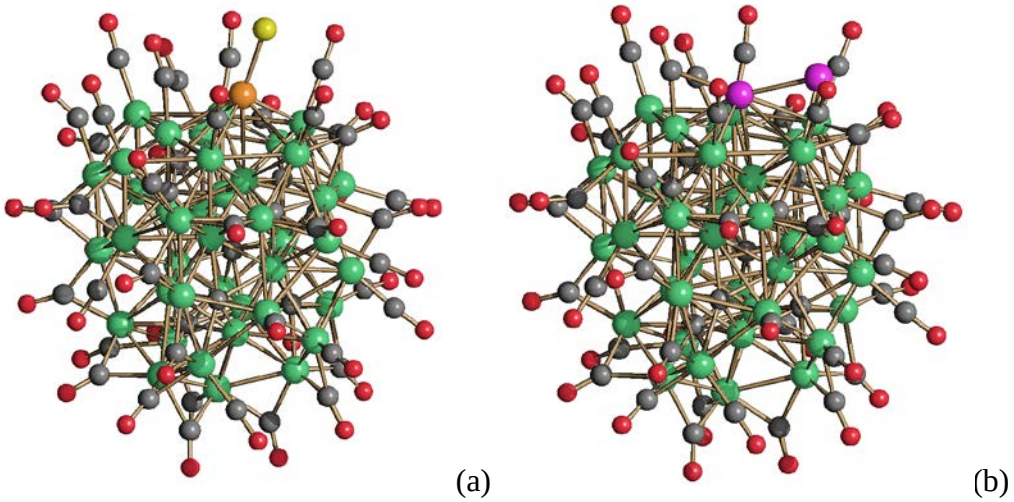

Fig. 16. Molecular structures of (a) $[HNi_{42}C_8(CO)_{44}(CuCl)]^{7-}$ and (b) $[HNi_{43+x}C_8(CO)_{45+x}]^{7-}$ (two CO ligands with partial occupancy factors have not been located) as found in $[NMe_4]_7[HNi_{42+2x}C_8(CO)_{44+2x}(CuCl)_{1-x}]\cdot 6.5MeCN$ (x = 0.14) (green, Ni; purple, Ni with partial occupancy factor; orange Cu; yellow, Cl; grey, C; red, O).

5.2.2 Nickel Carbide Carbonyl Clusters containing bonded C_2 units

Nickel based acetylide carbonyl clusters include both homometallic and heterometallic clusters (Figure 17), as well as mono-acetylide ($[Ni_{10}(C_2)(CO)_{16}]^{2-}$, $[Ni_{11}(C_2)(CO)_{15}]^{4-}$, $[Ni_{12}(C_2)(CO)_{16}]^{4-}$, $[Ni_2Co_6(C_2)(CO)_{16}]^{2-}$, $[Ni_2Co_6(C_2)(CO)_{14}(MeCN)_2]^{2-}$, $[Ni_9Co(C_2)(CO)_{16-x}]^{3-}$ (x = 0.58), $[Ni_7Co_3(C_2)(CO)_{16}]^{3-}$), bis-acetylide ($[Ni_{16}(C_2)_2(CO)_{23}]^{4-}$, $[Ni_{16+x}(C_2)_2(CO)_{23+x}]^{4-}$ (x = 0.12-0.96), $[Ni_6Rh_8(C_2)_2(CO)_{24}]^{4-}$) and tetra-acetylide ($[Ni_{22}(C_2)_4(CO)_{28}(Et_2S)]^{2-}$, $[H_{4-n}Ni_{25}(C_2)_4(CO)_{32}]^{n-}$ (n = 3, 4), $[Ni_{22}(C_2)_4(CO)_{28}Cl]^{3-}$, $[H_2Ni_{22}(C_2)_4(CO)_{28}(CdBr)_2]^{2-}$) species [86-88,104-107].

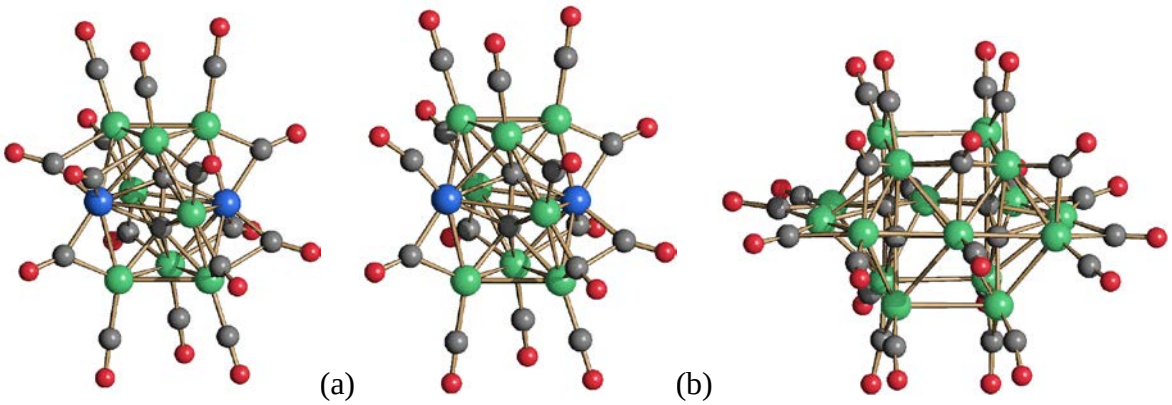

Fig. 17. Molecular structure of (a) $[Ni_9CoC_2(CO)_{16}]^{3-}$ and (b) $[Ni_9CoC_2(CO)_{15}]^{3-}$ as found in $[Ni_9Co(C_2)(CO)_{16-x}]^{3-}$ (x = 0.58); (c) $[Ni_{16}(C_2)_2(CO)_{23}]^{4-}$ (green, Ni; blue, Ni/Co; gray, C; red, O)

The C_2 units within these clusters display C-C bond distances in the range 1.368-1.493 Å. These values are intermediate between those of ethane (1.53 Å) and ethene (1.34 Å), suggesting a strong C-C interaction. Experimental and theoretical investigations point out that as the C-C interaction increases, the M-C interaction between the interstitial C atoms and the surrounding metal cage decreases. This is in keeping with the fact that often poly-acetylide clusters are less stable than poly-carbide clusters. Indeed, tightly bonded C_2 units seem less efficient than isolated carbide atoms in stabilizing MCCs, in view of the reduced interaction with the metal cage [104,105]. This might be somehow related to the proposed involvement of C_2 units in the growth of CNTs catalyzed by Ni, Co and Fe nanoparticles [114-117]. Indeed, we may speculate that, after formation of C atoms within a metal NP, the following formation of a C-C bond would weaken the interaction with the metal atoms and favors the segregation of the C_2 unit onto the surface, allowing the subsequent growth of more extended carbon frames.

All the tetra-acetylide MCCs so far reported contain interstitial $Ni(\eta^2\text{-}C_2)_4$, that is, $[H_{4-n}Ni_{25}(C_2)_4(CO)_{32}]^{n-}$ (n = 3, 4), or $Ni_2(\mu\text{-}\eta^2\text{-}C_2)_4$ units, that is, $[Ni_{22}(C_2)_4(CO)_{28}(Et_2S)]^{2-}$, $[Ni_{22}(C_2)_4(CO)_{28}Cl]^{3-}$ and $[H_2Ni_{22}(C_2)_4(CO)_{28}(CdBr)_2]^{2-}$ (Figure 18).

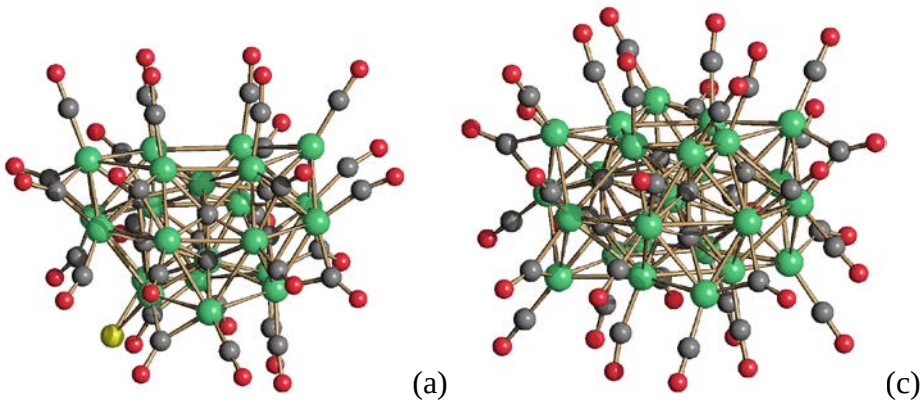

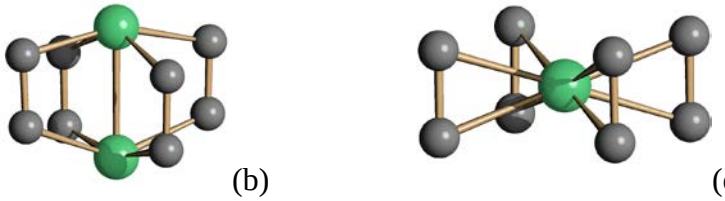

(b) (d)

Fig. 18. Molecular structures of (a) $[Ni_{22}(C_2)_4(CO)_{28}Cl]^{3-}$ and (b) its $Ni_2(\mu\text{-}\eta^2\text{-}C_2)_4$ interstitial unit, (c) $[Ni_{25}(C_2)_4(CO)_{32}]^{4-}$ and (d) its $Ni(\eta^2\text{-}C_2)_4$ unit (green, Ni; gray, C; red, O; yellow, Cl).

5.3 Electrochemical and Spectroscopic Properties of Nickel Carbide Carbonyl Clusters

As discussed in the previous sections, very often large MCCs display both reversible protonation/deprotonation and redox reactions. Thus, their charges can be changed in two ways: (1) addition/removal of H^+ ions *via* acid-base reactions; (2) addition/removal of electrons *via* redox reactions. The redox behavior of MCCs can be directly assessed by electrochemical and spectroelectrochemical (SEC) methods [40,118]. In particular, cyclic voltammetry (CV) and IR SEC are particularly suited for the study of multivalent MCCs. Electrochemical measurements are also an useful indication of the different ability of isolated C atoms and C_2 units to stabilize the cluster. Indeed, isolated C-atoms are very effective in stabilizing species with a different number of electrons and, thus, poly-carbide clusters undergo several reversible redox processes, e.g. $[Ni_{32}C_6(CO)_{36}]^{6-}$ (Figure 19) [119]. Conversely, C_2 units interact more weakly with the Ni cage and, thus, poly-acetylide clusters display poorer and less resolved cyclic voltammetries, as exemplified by $[HNi_{25}(C_2)_4(CO)_{32}]^{3-}$ [105].

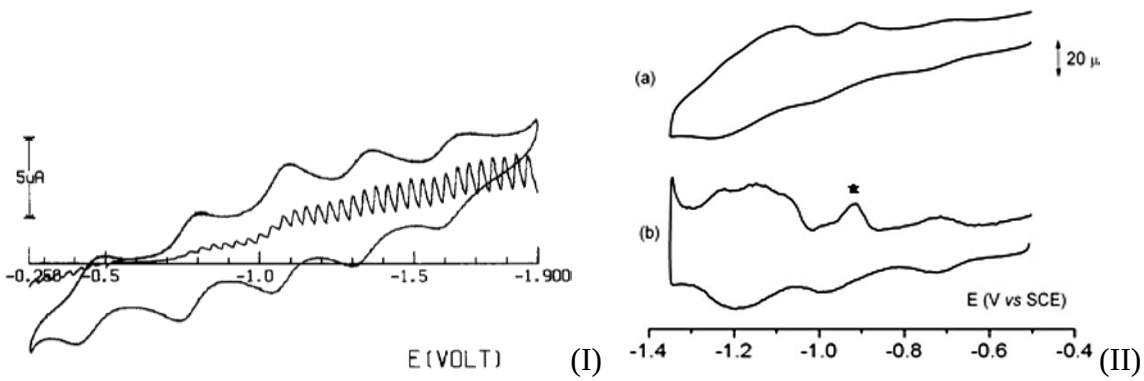

(I) (II)

Fig. 19. Voltammetric profiles of (I) $[Ni_{32}C_6(CO)_{36}]^{6-}$ and (II) $[HNi_{25}(C_2)_4(CO)_{32}]^{3-}$, cyclic (a) and first derivative deconvoluted (b) voltammograms. Reproduced with permission from ref. 105 and 119.

The hydride nature of lower nuclearity MCCs can be directly investigated by ^1H NMR spectroscopy and, sometimes, the hydride atoms directly located by SC-XRD. Alternatively, if larger crystals are available, single crystal neutron diffraction can be employed for the structural characterization of hydride clusters. It must be remarked that, due to the π-acidity of the CO ligands,

hydride ligands in transition metal carbonyl complexes and clusters behave as "protons" and, thus they are removed with bases and added with acids. Indeed, the archetypical $HCo(CO)_4$ behaves as a strong acid and easily dissociates into H^+ and $[Co(CO)_4]^-$.

As the nuclearity of MCCs increases, the assessment of hydrides becomes more complicated. Locating H-atoms by SC-XRD in the presence of an increasing number of heavy atoms becomes soon impossible. At the same time, growing larger crystals suitable for neutron diffraction is a hard task in the case of large MCCs (indeed also obtaining crystals suitable for SC-XRD is often very challenging). High nuclearity MCCs are not stable under ESI-MS conditions and, thus, also high-resolution mass spectrometry is not suitable for counting the H-atoms in poly-hydride MCCs. The most straightforward approach would be ^{1}H NMR spectroscopy but, in our experience, above a nuclearity of 20-30 metal atoms, MCCs seem to be NMR silent independently of the experimental conditions (concentration, solvent, temperature, spectrometer field, solution or solid state NMR, ^{1}H/^{2}D replacement and solution ^{2}D NMR) [88]. A satisfactory theoretical explanation for this phenomenon is not yet available, but it is likely to be the result of the combination of concomitant factors, such as dynamic site-exchange processes, insurgence of magnetism (in the ground and/or excited states), aggregation phenomena in solution.

The species $[H_{4-n}Ni_{22}(C_2)_4(CO)_{28}(CdBr)_2]^{n-}$ (n = 2-4) [88] and $[H_{8-n}Rh_{22}(CO)_{35}]^{n-}$ (n = 3-7) [120] are the largest MCCs, whose poly-hydride nature has been directly proved by ^{1}H NMR spectroscopy. In particular, the di-hydride di-anion $[H_2Ni_{22}(C_2)_4(CO)_{28}(CdBr)_2]^{2-}$ shows a broad resonance at δ_H –14 ppm which moves to δ_H –30 ppm upon deprotonation to the mono-hydride tri-anion $[HNi_{22}(C_2)_4(CO)_{28}(CdBr)_2]^{3-}$ (Figure 20). Further deprotonation affords the tetra-anion $[Ni_{22}(C_2)_4(CO)_{28}(CdBr)_2]^{4-}$ which does not show any hydride resonance, corroborating the presence and number of hydride ligands in the other two species. Variable temperature (VT) ^{1}H NMR experiments on solutions of $[H_{4-n}Ni_{22}(C_2)_4(CO)_{28}(CdBr)_2]^{n-}$ (n = 2-4) in different solvents clearly indicate the occurrence in solution of dynamic site-exchange processes. In addition, also the T-dependence of the chemical shift is quite surprising. For instance, for $[HNi_{22}(C_2)_4(CO)_{28}(CdBr)_2]^{3-}$ a drift of *ca.* 0.17 ppm K^{-1} and 0.21 ppm K^{-1} is measured in d^6-acetone and CD_3CN, respectively. This should be compared with a drift of less than 0.05 ppm K^{-1} for protons, unless if involved in hydrogen bonds. In the latter cases a drift of 0.1-0.5 ppm K^{-1} is observed.

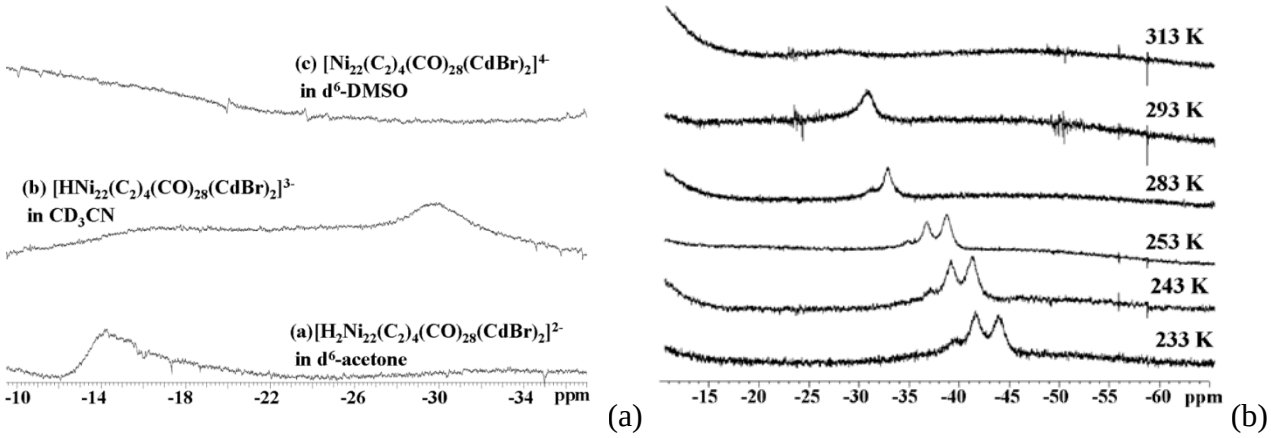

Fig. 20. (a) ^{1}H NMR spectra (400 MHz) recorded at 298 K of $[H_{4-n}Ni_{22}(C_2)_4(CO)_{28}(CdBr)_2]^{n-}$ (n = 2–4) in solvents of different basicity. (b) Variable temperature ^{1}H NMR spectra recorded at 600 MHz of $[HNi_{22}(C_2)_4(CO)_{28}(CdBr)_2]^{3-}$ in CD_3CN. Reproduced with permission from ref. 88.

Compared to $[H_{4-n}Ni_{22}(C_2)_4(CO)_{28}(CdBr)_2]^{n-}$ (n = 2-4), lower nuclearity MCCs such as $[H_{4-n}Ni_{12}(CO)_{21}]^{n-}$ (n = 2-4) show well resolved hydride resonances. Thus, it seems that as the size of the MCCs increases, the hydride resonances become broader and broader and, above a nuclearity of 20-30, they are lost in the baseline of the spectrum. At this point, only indirect proofs of the poly-hydride nature of MCCs can be obtained, including a combination of IR spectroscopy, electrochemical and spectroelectrochemical methods as well as SC-XRD analyses. Even if H-atoms cannot be located in larger clusters by SC-XRD, such analyses serve to determine the overall charge of the cluster by counting the counter-ions, beside showing that differently charged MCC anions are isostructural. IR spectroscopy further supports the occurrence of protonation/deprotonation equilibria in solution, by measuring the shift of the ν_{CO} frequencies upon addition of acids and bases. Finally, if the differently charged anions display identical redox properties, as determined by CV and IR SEC, they are the same compound to which has been added or removed one electron. Conversely, if their electrochemical properties are different, they must be different compounds, and the only difference should be the presence/absence of one H atom.

6. Conclusions

The chemistry of molecular Fe, Co and Ni carbide carbonyl clusters is very rich and diverse. In the case of Fe, this is dominated by the robust Fe_4C, Fe_5C and Fe_6C motives, which display a very attractive reactivity. In particular, the stability of such Fe-C environments is nowadays employed to develop Fe-S-C models of biological relevance [47-53].

From a structural point of view, the chemistry of Co carbide carbonyl clusters is richer than Fe, displaying more variegated structural motives, larger cluster sizes and the possibility of enclosing more C-atoms within the same molecular cage or even tightly bonded C_2-acetylide units. All these points are further enhanced in the case of Ni carbide clusters. Indeed, $[Ni_{45}C_{10}(CO)_{46}]^{6-}$ is the largest homometallic carbonyl cluster structurally characterized by SC-XRD reported to date. This is somehow related to the fact the number of valence electrons increases in the Fe-Co-Ni series, reducing the number of surface ligands required to stabilise the cluster. For instance, replacing Ni with Co in $[Ni_{45}C_{10}(CO)_{46}]^{6-}$ would require 68 CO ligands (assuming a 7- charge) in order to have an isoelectronic species. The required CO ligands would be 91 in order to replace Ni with Fe (assuming a 6- charge). It is clear that 68 or 91 CO ligands cannot be accommodated around a M_{45} cage. Because of this, Fe and Co clusters of such sizes have been not observed.

Beside the beauty and interest of their structures, carbide carbonyl clusters display some interesting chemical and physical properties. The enhanced stability conferred by interstitial carbide atoms favor the capacity of such clusters to undergo chemical reactions, such for instance the addition of S-atoms on their surface [47-53]. Similarly, often carbide clusters undergo reversible chemical and electrochemical redox reactions and, in the case of larger clusters, they behave as electron-sink and molecular nanocapacitors [11,40,58]. In addition, paramagnetism in both odd and even electron carbide carbonyl clusters has been documented, and a few examples have been included to the present mini-review.

Overall, the interest for molecular carbide carbonyl clusters spans different fields, such as bioinorganic chemistry [47-53], catalysis and electrocatalysis [54-57,73-77], applications of metal carbide nanoparticles [121] and models for the formation of C-C bonds within metal cages [112-117].

Appendix A. Supplementary material

Tables with the full list of clusters mentioned in this mini-review, with pertinent references and CCDC codes as .pdf file.

Acknowledgements

We gratefully thank the University of Bologna for financial support. We thank the referees for useful suggestions in revising the manuscript.

Conflicts of Interest. The authors declare no conflict of interest.

References

[1] E. H. Braye, L. F. Dahl, W. Hübel, D. L. Wampler, The Preparation, Properties and Structure of the Iron Carbonyl Carbide $Fe_5(CO)_{15}C$, J. Am. Chem. Soc. 84 (1962) 4633-4639.

[2] A. Sirigu, M. Bianchi, E. Benedetti, The Crystal Structure of $Ru_6C(CO)_{17}$, Chem. Commun. (1969) 596.

[3] C. R. Eady, B. F. G. Johnson, J. Lewis, The Chemistry of Polynuclear Compounds. Part XXVI. Products of the Pyrolysis of Dodecacarbonyl-*triangulo*-triruthenium and -triosmium, J. Chem. Soc., Dalton. Trans. (1975), 2606-2611.

[4] A. Reinholdt, J. Bendix, Transition Metal Carbide Complexes, Chem. Rev. 122 (2022), 830-902.

[5] R. D. Adams, H. Akter, M. D. Smith, C–C coupling of ethyne to the carbido ligand in products from reactions with $Ru_5(\mu_5\text{-}C)(CO)_{15}$, J. Organomet. Chem. 961 (2022) 122262.

[6] S. Takemoto, H. Matsuzaka, Recent advances in the chemistry of ruthenium carbido complexes, Coord. Chem. Rev. 256 (2012), 574-588.

[7] C. K. Barik, R. Ganguly, Y. Li, S. Samanta, W. K. Leong, Reaction of the Decaosmium Carbido Cluster $[Os_{10}(\mu_6\text{-}C)(CO)_{24}]^{2-}$ with Halostibines, J. Clust. Sci. 32 (2021) 929-935.

[8] C. Li, J. Xu, J. Zhao, D. Tian, R. B. King, The maximum number of carbonyl groups around an Ru_6C polyhedral cluster: hexanuclear ruthenium carbonyl carbides, Dalton Trans. 39 (2010) 10697-10701.

[9] J. Zhao, J. Xu, R. B. King, Hexanuclear Cobalt Carbonyl Carbide Clusters: The Interplay between Octahedral and Trigonal Prismatic Structures, Inorg. Chem. 47 (2008) 9314-9320.

[10] W. Buchowicz, B. Herbaczyńska, L. B. Jerzykiewicz, T. Lis, S. Pasynkiewicz, A. Pietrzykowski, Triple C-H Bond Activation of a Nickel-Bound Methyl Group: Synthesis and X-Ray Structure of a Carbide Cluster $(NiCp)_6(\mu_6\text{-}C)$, Inorg. Chem. 51 (2012) 8292-8297.

[11] C. Cesari, J.-H. Shon, S. Zacchini, L. A. Berben, Metal carbonyl clusters of groups 8-10: synthesis and catalysis, Chem. Soc. Rev. 50 (2021) 9503-9539.

[12] J. H. Davis, M. A. Beno, J. M. Williams, J. Zimmie, M. Tachikawa, E. L. Muetterties, Structure and chemistry of a metal cluster with a four-coordinate carbide carbon atom, Proc. Nat. Acad. Sci. 78 (1981) 668-671.

[13] J. S. Bradley, The Chemistry of Carbidocarbonyl Clusters, Adv. Organomet. Chem. 22 (1983) 1-58.

[14] J. S. Bradley, Carbidocarbonyl clusters of iron, Phil. Trans. R. Soc. Lond. A 308 (1982) 103-113.

[15] M. Tachikawa, E. L. Muetterties, Metal Carbide Clusters, Prog. Inorg. Chem. 28 (1981) 203-238.

[16] J. S. Bradley, S. Harris, J. M. Newsam, E. W. Hill, S. Leta, M. A. Modrick, Syntheses and Molecular and Electronic Structures of the μ_4-Methylidyne Clusters $[Fe_4(CO)_{12}C\text{-}C(O)OCH_3]^-$ and $[Fe_4(CO)_{12}C\text{-}C(CH_3)]^-$: an Analysis of Steric and Bonding Effects, Organometallics 6 (1987) 2060-2069.

[17] M. Tachikawa, E. L. Muetterties, Metal Clusters. 25. A uniquely bonded C-H group and reactivity of a low-coordinate carbidic carbon atom, J. Am. Chem. Soc. 102 (1980) 4541-4542.

[18] M. Tachikawa, R. L. Geerts, E. L. Muetterties, Metal Carbide Clusters Synthesis Systematics for Heteronuclear Species, J. Organomet. Chem. 213 (1981) 11-24.

[19] E. L. Muetterties, T. N. Rhodin, E. Band, C. F. Bruker, W. R. Pretzer, Clusters and Surfaces, Chem. Rev. 79 (1979) 91-137.

[20] E. L. Muetterties, J. Stein, Mechanistic Features of Catalytic Carbon Monoxide Hydrogenation Reactions, Chem. Rev. 79 (1979) 479-490.

[21] P. M. Maitlis, V. Zanotti, The role of electrophilic species in the Fischer-Tropsch reaction, Chem. Commun. (2009) 1619-1634.

[22] I. T. Moraru, L. M. Martínez-Prieto, Y. Coppet, B. Chaudret, L. Cusinato, I. del Rosal, R. Poteau, A combined theoretical/experimental study highlighting the formation of carbides on Ru nanoparticles during CO hydrogenation, Nanoscale 13 (2021) 6902-6915.

[23] Q.-Y. Liu, C. Shang, Z.-P. Liu, *In Situ* Active Site for CO Activation in Fe-Catalyzed Fischer-Tropsch Synthesis from Machine Learning, J. Am. Chem. Soc. 143 (2021) 11109-11120.

[24] J. Ohata, A. Teramoto, H. Fijita, S. Takemoto, H. Matsuzaka, Linear Hydrocarbon Chain Growth From a Molecular Diruthenium Carbide Platform, J. Am. Chem. Soc. 143 (2021) 16105-16112.

[25] Y. Jiao, H. Ma, H. Wang, Y.-W. Li, X.-D. Wen, H. Jiao, Interactive network of the dehydrogenation of alkanes, alknes and alkynes - surface carbon hydrogenative coupling on Ru(111), Catal. Sci. Technol. 11 (2021) 191-210.

[26] J. M. H. Lo, T. Ziegler, Theoretical Studies of the Formation and Reactivity of C2 Hydrocarbon Species on the Fe(100) Surface, J. Phys. Chem. C 122 (2018) 15505-15519.

[27] H. Schulz, Short history and present trends of Fischer-Tropsch synthesis, Applied Catalysis A: General 189 (1999) 3-12.

[28] C. K. Rofer-DePoorter, A Comprehensive Mechanism for the Fischer-Tropsch Synthesis, Chem. Rev. 81 (1981) 447-474.

[29] N. M. West, A. J. M. Miller, J. A. Labinger, J. E. Bercaw, Homogeneous Syngas Conversion, Coord. Chem. Rev. 255 (2011) 881-898.

[30] P. Braunstein, L. A. Oro, P. R. Raithby (Eds.), Metal Clusters in Chemistry, Wiley-VCH, Weinheim, 1999.

[31] G. Schmid (Ed.), Clusters and Colloids, Wiley-VCH, Weinheim, 1994.

[32] P. F. Jackson, B. F. G. Johnson, J. Lewis, M. McPartlin, W. J. H. Nelson, $H_2Ru_6(CO)_{18}$, $[HRu_6(CO)_{18}]^-$, and $[Ru_6(CO)_{18}]^{2-}$: a simple high yield route to these clusters and the X-ray structure of $[Ph_3MeP]_2[Ru_6(CO)_{18}]$, J. Chem. Soc., Chem. Commun. (1979) 735-736.

[33] B. F. G. Johnson, J. Lewis, S. W. Sankey, K. Wong, M. McPartlin, W. J. H. Nelson, An improved synthesis of the hexaruthenium carbido cluster $Ru_6C(CO)_{17}$; X-ray structure of the salt $[Ph_4As]_2[Ru_6C(CO)_{16}]$, J. Organomet. Chem. 191 (1980) C3-C7.

[34] M. R. Churchill, J. Wormald, J. Knight, M. J. Mays, Synthesis and Crystallographic Characterization of $[Me_4N^+]_2[Fe_6(CO)_{16}C^{2-}]$, a Hexanuclear Carbidocarbonyl Derivative of Iron, J. Am. Chem. Soc. 93 (1971) 3073-3074.

[35] A. Bernardi, I. Ciabatti, C. Femoni, M. C. Iapalucci, G. Longoni, S. Zacchini, Molecular nickel poly-carbide carbonyl nanoclusters: The octa-carbide $[HNi_{42}C_8(CO)_{44}(CuCl)]^{7-}$ and the deca-carbide $[Ni_{45}C_{10}(CO)_{46}]^{6-}$, J. Organomet. Chem. 812 (2016) 229-239.

[36] R. Jin, C. Zeng, M. Zhou, Y. Chen, Atomically Precise Colloid Metal Nanoclusters and Nanoparticles: Fundamentals and Opportunities, Chem. Rev. 116 (2016) 10346-10413.

[37] Y. Li, M. Zhou, R. Jin, Programmable Metal Nanoclusters with Atomic Precision, Adv. Mater. 33 (2021) 2006591.

[38] R. Jin, G. Li, S. Sharma, Y. Li, X. Du, Toward Active-Site Tailoring in Heterogeneous Catalysis by Atomically Precise Metal Nanoclusters with Crystallographic Structures, Chem. Rev. 121 (2021) 567-648.

[39] T. Kawawaki, Y. Imai, D. Suzuki, S. Kato, I. Kobayashi, T. Suzuki, R. Kaneko, S. Hossain, Y. Negishi, Atomically Precise Alloy Nanoclusters, Chem. Eur. J. 26 (2020) 16150-16193.

[40] C. Femoni, M. C. Iapalucci, F. Kaswalder, G. Longoni, S. Zacchini, The possible role of metal carbonyl clusters in nanoscience and nanotechnologies, Coord. Chem. Rev. 250 (2006) 1580-1604.

[41] K. M. Lancaster, M. Roemelt, P. Ettenhuber, Y. Hu, M. W. Ribbe, F. Neese, U. Bergmann, S. DeBeer, X-ray Emission Spectroscopy Evidences a Central Carbon in the Nitrogenase Iron-Molybdenum Cofactor, Science 334 (2011) 974-977.

[42] T. Spatzal, M. Aksoyoglu, L. Zhang, S. L. A. Andrade, E. Schleicher, S. Weber, D. C. Rees, O. Einsle, Evidence for Interstitial Carbon in Nitrogenase FeMo Cofactor, Science 334 (2011) 940-940.

[43] J. A. Rees, R. Bjornsson, J. Schlesier, D. Sippel, O. Einsle, S. DeBeer, The Fe-V a Cofactor of Vanadium Nitrogenase Contains an Interstitial Carbon Atom, Angew. Chem. Int. Ed. 54 (2015) 13249-13252.

[44] Y. Hu, M. W. Ribbe, Nitrogenase - A Tale of Carbon Atom(s), Angew. Chem. Int. Ed. 55(2016) 8216-8226.

[45] T. M. Buscagan, K. A. Perez, A. O. Maggiolo, D. C. Rees, T. Spatzal, Structural Characterization of Two CO Molecules Bound to the Nitrogenase Active Site, Angew. Chem. Int. Ed. 60 (2021) 5704-5707.

[46] I. Čorić, P. L. Holland, Insight into the Iron-Molybdenum Cofactor of Nitrogenase from Synthetic Iron Complexes with Sulfur, Carbon, and Hydride Ligands, J. Am. Chem. Soc. 138 (2016) 7200-7211.

[47] C. Joseph, C. R. Cobb, M. J. Rose, Single-Step Sulfur Insertion into Iron Carbide Carbonyl Clusters: Unlocking the Synthetic Door to FeMoco Analogues, Angew. Chem. Int. Ed. 60 (2021) 3433-3437.

[48] C. Joseph, J. P. Shupp, C. R. Cobb, M. J. Rose, Construction of Synthetic Models for Nitrogenase-Relevant NifB Biogenesis Intermediates and Iron-Carbide-Sulfide Clusters, Catalysts 10 (2020) 1317.

[49] J. McGale, G. E. Cutsail, C. Joseph, M. J. Rose, S. Debeer, Spectroscopic X-ray and Mössbauer Characterization of M_6 and M_5 Iron(Molybdenum)-Carbonyl Carbide Clusters: High Carbide-Iron Covalency Enhances Local Iron Site Electron Density despite Cluster Oxidation, Inorg. Chem. 58 (2019) 12918-12932.

[50] C. Joseph, S. Kuppuswamy, V. M. Lynch, M. J. Rose, Fe_5Mo Cluster with Iron-Carbide and Molybdenum-Carbide Bonding Motifs: Structure and Selective Alkyne Reductions, Inorg. Chem. 57 (2018) 20-23.

[51] S. Kuppuswamy, J. D. Wofford, C. Joseph, Z.-L. Xie, A. K. Ali, V. M. Lynch, P. A. Lindahl, M. J. Rose, Structures, Interconversions, and Spectroscopy of Iron Carbonyl Clusters with an Interstitial Carbide: Localized Metal Center Reduction by Overall Cluster Oxidation, Inorg. Chem. 56 (2017) 5998-6012.

[52] L. Liu, T. J. Woods, T. B. Rauchfuss, Reactions of $[Fe_6C(CO)_{14}(S)]^{2-}$: Cluster Growth, Redox, Sulfiding, Eur. J. Inorg. Chem. (2020) 3460-3465.

[53] L. Liu, T. B. Rauchfuss, T. J. Woods, Iron Carbide-Sulfide Carbonyl Clusters, Inorg. Chem. 58 (2019) 8271-8274.

[54] S. Pattanayak, L. A. Berben, Cobalt Carbonyl Clusters Enable Independent Control of Two Proton Transfer Rates in the Mechanism for Hydrogen Evolution, ChemElectroChem 8 (2021) 2488-2494.

[55] C. R. Carr, A. Taheri, L. A. Berben, Fast Proton Transfer and Hydrogen Evolution Reactivity Mediated by $[Co_{13}C_2(CO)_{24}]^{4-}$, J. Am. Chem. Soc. 142 (2020) 12299-12305.

[56] A. Taheri, L. A. Berben, Tailoring Electrocatalysts for Selective CO_2 and H^+ Reduction: Iron Carbonyl Clusters as a Case Study, Inorg. Chem. 55 (2016) 378-385.

[57] A. D. Nguyen, M. Diego Rail, M. Shanmugam, J. C. Fettinger, L. A. Berben, Electrocatalytic Hydrogen Evolution from Water by a Series of Iron Carbonyl Clusters, Inorg. Chem. 52 (2013) 12847-12854.

[58] S. Zacchini, Using Metal Carbonyl Clusters To Develop a Molecular Approach towards Metal Nanoparticles, Eur. J. Inorg. Chem. (2011) 4125-4145.

[59] A. V. Virovets, E. Peresypkina, M. Scheer, Structural Chemistry of Giant Metal Based Supramolecules, Chem. Rev. 121 (2021) 14485-14554.

[60] G. Longoni, A. Ceriotti, R. Della Pergola, M. Manassero, M. Perego, G. Piro, M. Sansoni, Iron, cobalt and nickel carbide-carbonyl clusters by CO scission, Philos. Trans. R. Soc. A 308 (1982) 47-57.

[61] G. Hogarth, S. E. Kabir, E. Nordlander, Cluster chemistry in the Noughties: new developments and their relationship to nanoparticles, Dalton Trans. 39 (2010) 6153-6174.

[62] C. Femoni, C. Cesari, M. C. Iapalucci, S. Ruggieri, S. Zacchini, Group 9 and 10 Carbonyl Clusters, Reference Module in Chemistry, Molecular Science and Chemical Engineering, Elsevier (2022) ISBN 9780124095472.

[63] J. S. Bradley, G. B. Ansell, M. E. Leonowicz, E. W. Hill, Synthesis and Molecular Structure of μ^4-Carbido-μ^2-carbonyl-dodecacarbonyltetrairon, a Neutral Iron Butterfly Cluster Bearing and Exposed Carbon Atom, J. Am. Chem. Soc. 103 (1981) 4968-4970.

[64] E. M. Holt, K. H. Whitmire, D. F. Shriver, The role of metal cluster interactions in the proton-induced reduction of CO. The crystal structures of [PPN][$HFe_4(CO)_{12}C$] and $HFe_4(CO)_{12}(\eta^2$-$COCH_3$), J. Organomet. Chem. 213 (1981) 125-137.

[65] M. A. Beno, J. M. Williams, M. Tachikawa, E. L. Muetterties, Fischer-Tropsch Chemistry: Structure of a Seminal η^2-CH Cluster Derivative, $HFe_4(\eta^2$-$CH)(CO)_{12}$, J. Am. Chem. Soc. 102 (1980) 4542-4544.

[66] A. Gourdon, Y. Jeannin, Electrochemistry and X-ray structures of the isoelectronic clusters $[Fe_5C(CO)_{15}]$, $[N(PPh_3)_2][Fe_5N(CO)_{14}]$ and $[NBu_4]_2[Fe_5C(CO)_{14}]$, J. Organomet. Chem. 290 (1985) 199-211.

[67] M. Bortoluzzi, I. Ciabatti, C. Cesari, C. Femoni, M. C. Iapalucci, S. Zacchini, Synthesis of the Highly Reduced $[Fe_6C(CO)_{15}]^{4-}$ Carbonyl Carbide Cluster and Its Reactions with H^+ and $[Au(PPh_3)]^+$, Eur. J. Inorg. Chem. (2017) 3135-3143.

[68] I. Ciabatti, C. Femoni, M. Hayatifar, M. C. Iapalucci, I. Maggiore, S. Stagni, S. Zacchini, Bimetallic Fe-Cu Carbido Carbonyl Clusters Obtained from the Reactions of $[Fe_4C(CO)_{12}\{Cu(MeCN)\}_2]$ with N-Donor Ligands, J. Clust. Sci. 27 (2016) 431-456.

[69] R. Della Pergola, A. Sironi, L. Garlaschelli, D. Strumolo, C. Manassero, M. Manassero, S. Fedi, P. Zanello, F. Kaswalder, S. Zacchini, Fe-Cu octahedral carbide clusters, and the replacement of their labile halide ligands: Synthesis, solid state structure, substitution and electrochemical reactivity of $[Fe_5C(CO)_{14}(CuBr)]^{2-}$, $[Fe_4C(CO)_{12}(CuCl)_2]^{2-}$, $[\{Fe_4Cu_2C(CO)_{12}(\mu\text{-}Cl)\}_2]^{2-}$, $[Fe_5C(CO)_{14}(CuOC_4H_8)]^-$ and $[Fe_4C(CO)_{12}(CuNCMe)_2]$, Inorg. Chim. Acta 363 (2010) 586-594.

[70] C. Femoni, R. Della Pergola, M. C. Iapalucci, F. Kaswalder, M. Riccò, S. Zacchini, Copolymerization of $Fe_4Cu_2C(CO)_{12}$ moieties with bidentate N-ligands: synthesis and crystal structure of the $[Fe_4Cu_2(\mu_6\text{-}C)(CO)_{12}(\mu\text{-bipy})]_4 \cdot 8THF$ square tetramer and the infinite $[Fe_4Cu_2(\mu_6\text{-}C)(CO)_{12}(\mu\text{-L–L})]_\infty$ zigzag chains, Dalton Trans. (2009) 1509-1511.

[71] R. Della Pergola, A. Sironi, A. Rosehr, V. Colombo, A. Sironi, N-Heterocyclic carbene copper complexes tethered to iron carbidocarbonyl clusters, Inorg. Chem. Commun. 49 (2014) 27-29.

[72] R. Della Pergola, A. Sironi, M. Moret, S. Bergantin, P. R. Mussini, M. Panigati, Cyclic dimers of variable size, formed from FeCu carbide clusters: Synthesis, structure and electrochemical behaviour of $[\{Fe_4C(CO)_{12}Cu_2(\mu\text{-}X)\}_2]^{n-}$, (X = phenylthiolate, pyrazolate, (n = 2) or diphenolate (n = 4)), J. Organomet. Chem. 728 (2013) 23-29.

[73] M. Diego Rail, L. A. Berben, Directing the reactivity of $[HFe_4N(CO)_{12}]^-$ toward H^+ or CO_2 reduction by understanding the electrocatalytic mechanism, J. Am. Chem. Soc. 133 (2011) 18577-18579.

[74] N. D. Loewen, T. V. Neelakantam, L. A. Berben, Renewable Formate from C-H Bond Formation with CO_2: Using Iron Carbonyl Clusters as Electrocatalysts, Acc. Chem. Res. 50 (2017) 2362-2370.

[75] A. Taheri, L. A. Berben, Making C-H bonds with CO_2: production of formate by molecular electrocatalysts, Chem. Commun. 52 (2016) 1768-1777.

[76] A. Taheri, C. R. Carr, L. A. Berben, Electrochemical methods for assessing kinetic factors in the reduction of CO_2 to Formate: Implications for improving electrocatalyst design, ACS Catal. 8 (2018) 5787-5793.

[77] H. Jang, Y. Qiu, M. E. Hutchings, M. Nguyen, L. A. Berben, L.-P. Wang, Quantum chemical studies of redox properties and conformational changes of a four-center iron CO_2 reduction electrocatalyst, Chem. Sci. 9 (2018) 2645-2654.

[78] I. Ciabatti, C. Femoni, M. Hayatifar, M. C. Iapalucci, G. Longoni, C. Pinzino, M. V. Solmi, S. Zacchini, The Redox Chemistry of $[Co_6C(CO)_{15}]^{2-}$: A Synthetic Route to New Co-Carbide Carbonyl Clusters, Inorg. Chem. 53 (2014) 3818-3831.

[79] S. Martinengo, D. Strumolo, P. Chini, D. Braga, New carbide clusters in the cobalt subgroup. Part 13. Synthesis and chemical characterization of the anions $[Co_6C(CO)_{14}]^-$, $[Co_6C(CO)_{15}]^{2-}$, and $[Co_8C(CO)_{18}]^{2-}$, and crystal structure of μ_6-carbido-ennea-μ-carbonyl-hexacarbonyl-*polyhedro*-hexacobaltate(2–) as its benzyltrimethylammonium salt; a comparison with isostructural species, J. Chem. Soc., Dalton Trans. (1985) 35-41.

[80] V. G. Albano, P. Chini, G. Ciani, M. Sansoni, S. Martinengo, New carbide clusters in the cobalt sub-group. Part 6. Crystallographic characterization of the tetramethylammonium salt of the paramagnetic anion carbidohexa-m-carbonyl-octacarbonyl-*polyhedro*-hexa-cobaltate(1–), J. Chem. Soc., Dalton Trans. (1980) 163-166.

[81] A. Fumagalli, M. Costa, R. Della Pergola, P. Zanello, F. Fabrizi de Biani, P. Macchi, A. Sironi, Synthesis, structural and electrochemical characterization of the nitrido-carbonyl cluster anion $[Co_{13}N_2(CO)_{24}]^{3-}$. The different redox propensity of the two isostructural families $[Co_{13}N_2(CO)_{24}]^{n-}$ and $[Co_{13}C_2(CO)_{24}]^{m-}$, Inorg. Chim. Acta 350 (2003) 187-192.

[82] S. Martinengo, L. Noziglia, A. Fumagalli, V. G. Albano, D. Braga, F. Grepioni, Synthesis and structural characterization of the dianion $[Co_9(C_2)(CO)_{19}]^{2-}$ as its tetramethylammonium salt, J. Chem. Soc., Dalton Trans. (1998) 2493-2496.

[83] A. Ceriotti, R. Della Pergola, G. Longoni, M. Manassero, N. Masciocchi, M. Sansoni, Bimetallic Co-Ni carbide clusters: synthesis and crystal structure of the $[Co_2Ni_{10}(CO)_{20}C]^{2-}$ and $[Co_3Ni_9(CO)_{20}C]^{2-}$ dianions, J. Organomet. Chem. 330 (1987) 237-252.

[84] A. Arrigoni, A. Ceriotti, R. Della Pergola, G. Longoni, M. Manassero, M. Sansoni, Synthesis and chemical behavior of the $[Co_3Ni_7(CO)_{16}C_2]^{2-}$ and $[Co_3Ni_7(CO)_{15}C_2]^{3-}$ dicarbide clusters; X-ray crystal structure of $[PPh_4]_2[Co_3Ni_7(CO)_{16}C_2]$, J. Organomet. Chem. 296 (1985) 243-253.

[85] A. Arrigoni, A. Ceriotti, R. Della Pergola, G. Longoni, M. Manassero, N. Masciocchi, M. Sansoni, Synthesis and Crystal Structure of the Dicarbido Bimetallic Cluster $[Co_6Ni_2C_2(CO)_{16}]^{2-}$, Angew. Chem. Int. Ed. 23 (1984) 322-323.

[86] I. Ciabatti, C. Femoni, M. C. Iapalucci, G. Longoni, S. Zacchini, Bimetallic Nickel-Cobalt Hexacarbido Carbonyl Clusters $[H_{6-n}Ni_{22}Co_6C_6(CO)_{36}]^{n-}$ (n = 3-6) Possessing Polyhydride

Nature and Their Base-Induced Degradation to the Monoacetylide $[Ni_9CoC_2(CO)_{16-x}]^{3-}$ (x = 0, 1), Organometallics 31 (2012) 4593-4600.

[87] I. Ciabatti, F. Fabrizi de Biani, C. Femoni, M. C. Iapalucci, G. Longoni, S. Zacchini, Selective synthesis of the $[Ni_{36}Co_8C_8(CO)_{48}]^{6-}$ octa-carbide carbonyl cluster by thermal decomposition of the $[H_2Ni_{22}Co_6C_6(CO)_{36}]^{4-}$ hexa-carbide, Dalton Trans. 42 (2013) 9662-9670.

[88] A. Bernardi, C. Femoni, M. C. Iapalucci, G. Longoni, S. Zacchini, The problems of detecting hydrides in metal carbonyl clusters by ^1H NMR: the case study of $[H_{4-n}Ni_{22}(C_2)_4(CO)_{28}(CdBr)_2]^{n-}$ (n = 2-4), Dalton Trans. (2009) 4245-4251.

[89] C. Femoni, M. C. Iapalucci, G. Longoni, J. Wolowska, S. Zacchini, P. Zanello, S. Fedi, M. Riccò, D. Pontiroli, M. Mazzani, Magnetic Behavior of Odd- and Even-Electron Metal Carbonyl Clusters: The Case Study of $[Co_8Pt_4C_2(CO)_{24}]^{n-}$ (n = 2, 2) Carbide Cluster, J. Am. Chem. Soc. 132 (2010) 2919-2927.

[90] I. Ciabatti, F. Fabrizi de Biani, C. Femoni, M. C. Iapalucci, G. Longoni, S. Zacchini, Metal Segregation in Bimetallic Co-Pd Carbide Carbonyl Clusters: Synthesis, Structure, Reactivity and Electrochemistry of $[H_{6-n}Co_{20}Pd_{16}C_4(CO)_{48}]^{n-}$ (n = 3-6), ChemPlusChem 78 (2013) 1456-1465.

[91] C. Femoni, M. C. Iapalucci, G. Longoni, S. Zacchini, S. Fedi, F. Fabrizi de Biani, Cage Rearrangements in Dodecanuclear Co-Pt Dicarbido Clusters Promoted by Redox Reactions, Eur. J. Inorg. Chem. (2012) 2243-2250.

[92] M. P. Cifuentes, M. G. Humphrey, J. E. McGrady, P. J. Smith, R. Stranger, K. S. Murray, B. Moubaraki, High Nuclearity Ruthenium Carbonyl Cluster Chemistry. 5. Local Density Functional, Electron Spectroscopy, Magnetic Susceptibility, and Electron Paramagnetic Resonance Studies on (Carbido)decaruthenium Carbonyl Clusters, J. Am. Chem. Soc. 119 (1997) 2647-2655.

[93] I. Ciabatti, C. Femoni, M. Gaboardi, M. C. Iapalucci, G. Longoni, D. Pontiroli, M. Riccò, S. Zacchini, Structural rearrangements induced by acid-base reactions in metal carbonyl clusters: the case of $[H_{3-n}Co_{15}Pd_9C_3(CO)_{38}]^{n-}$ (n = 0-3), Dalton Trans. 43 (2014) 4388-4399.

[94] B. Berti, I. Ciabatti, C. Femoni, M. C. Iapalucci, S. Zacchini, Cluster Core Isomerism Induced by Crystal Packing Effects in the $[HCo_{15}Pd_9C_3(CO)_{38}]^{2-}$ Molecular Nanocluster, ACS Omega 3 (2018) 13239-13250.

[95] C. Cesari, B. Berti, F. Calcagno, C. Femoni, M. Garavelli, M. C. Iapalucci, I. Rivalta, S. Zacchini, Polymerization Isomerism in Co-M (M = Cu, Ag, Au) Carbonyl Clusters: Synthesis, Structures and Computational Investigation, Molecules 26 (2021) 1529.

[96] W. W. Xu, X. C. Zeng, Y. Gao, The structural isomerism in gold nanoclusters, Nanoscale 10 (2018) 9476-9483.

[97] R. Reina, O. Riba, O. Rossell, M. Seco, D. de Montauzon, M. A. Pellinghelli, A. Tiripicchio, M. Font-Bardía, X. Solans, Mixed cobalt/gold clusters based on octahedral or prismatic Co_6C skeletons, J. Chem. Soc., Dalton Trans. (2000) 4464-4469.

[98] I. Ciabatti, C. Femoni, M. Hayatifar, M. C. Iapalucci, S. Zacchini, Co_5C and Co_4C carbido carbonyl clusters stabilized by $[AuPPh_3]^+$, Inorg. Chim. Acta 428 (2015) 203-211.

[99] I. Ciabatti, C. Femoni, M. Hayatifar, M. C. Iapalucci, A. Ienco, G. Longoni, G. Manca, S. Zacchini, Octahedral Co-Carbide Carbonyl Clusters Decorated by $[AuPPh_3]^+$ Fragments: Synthesis, Structural Isomerism, and Aurophilic Interactions of $Co_6C(CO)_{12}(AuPPh_3)_4$, Inorg. Chem. 53 (2014) 9761-9770.

[100] M. Bortoluzzi, I. Ciabatti, C. Femoni, T. Funaioli, M. Hayatifar, M. C. Iapalucci, G. Longoni, S. Zacchini, Homoleptic and heteroleptic Au(I) complexes containing the new $[Co_5C(CO)_{12}]^-$ cluster as ligand, Dalton Trans. 43 (2014) 9633-9646.

[101] A. F. Masters, J. T. Meyer, Structural systematics in nickel carbonyl cluster anions, Polyhedron 14 (1995) 339-365.

[102] J. K. Beattie, A. F. Masters, J. T. Meyer, Nickel carbonyl cluster complexes, Polyhedron 14 (1995) 829-868.

[103] C. Cesari, I. Ciabatti, C. Femoni, M. C. Iapalucci, S. Zacchini, Capping $[H_{8-n}Ni_{42}C_8(CO)_{44}]^{n-}$ (n = 6, 7, 8) Octa-carbide Carbonyl Nanoclusters with [Ni(CO)] and [CuCl] Fragments, J. Clust. Sci. 28 (2017) 1963-1979.

[104] C. Femoni, M. C. Iapalucci, G. Longoni, S. Zacchini, S. Fedi, F. Fabrizi de Biani, Nickel poly-acetylide carbonyl clusters: structural features, bonding and electrochemical behaviour, Dalton Trans. 41 (2012) 4649-4663.

[105] C. Femoni, M. C. Iapalucci, G. Longoni, S. Zacchini, Polycarbide nickel clusters containing interstitial $Ni(\eta_2\text{-}C_2)_4$ and $Ni_2(\mu\text{-}\eta^2\text{-}C_2)_4$ acetylide moieties: mimicking the supersaturated Ni-C solutions preceding the catalytic growth of CNTs with the structures of $[HNi_{25}(C_2)_4(CO)_{32}]^{3-}$ and $[Ni_{22}(C_2)_4(CO)_{28}Cl]^{3-}$, Chem. Commun. (2008) 3157-3159.

[106] I. Ciabatti, C. Femoni, T. Funaioli, M. C. Iapalucci, S. Merighi, S. Zacchini, The redox chemistry of $[Ni_9C(CO)_{17}]^{2-}$ and $[Ni_{10}(C_2)(CO)_{16}]^{2-}$: Synthesis, electrochemistry and structure of $[Ni_{12}C(CO)_{18}]^{4-}$ and $[Ni_{22}(C_2)_4(CO)_{28}(Et_2S)]^{2-}$, J. Organomet. Chem. 849-850 (2017) 299-305.

[107] C. Femoni, M. C. Iapalucci, G. Longoni, S. Zacchini, Hetero-Bimetallic Ni-Rh Carbido Carbonyl Clusters: Synthesis, Structure and ^{13}C NMR of $[Ni_{10}Rh_2C(CO)_{20}]^{2-}$, $[Ni_9Rh_3C(CO)_{20}]^{3-}$ and $[Ni_6Rh_8(C_2)_2(CO)_{24}]^{4-}$, Eur. J. Inorg. Chem. (2009) 2487-2495.

[108] A. Bernardi, I. Ciabatti, C. Femoni, M. C. Iapalucci, G. Longoni, S. Zacchini, Ni-Cu tetracarbide carbonyls with vacant Ni(CO) fragments as borderline compounds between molecular and quasi-molecular clusters, Dalton Trans. 42 (2013) 407-421.

[109] A. Bernardi, C. Femoni, M. C. Iapalucci, G. Longoni, S. Zacchini, S. Fedi, P. Zanello, Synthesis, Structures and Electrochemistry of New Carbonylnickel Octacarbide Clusters: The Distorting Action of Carbide Atoms in the Growth of Ni Cages and the First Example of the Inclusion of a Carbon Atom within a (Distorted) Ni Octahedral Cage, Eur. J. Inorg. Chem. (2010) 4831-4842.

[110] A. Bernardi, C. Femoni, M. C. Iapalucci, G. Longoni, S. Zacchini, Cadmium-substitution promoted by nucleophilic attack of $[Ni_{30}C_4(CO)_{34}(CdX)_2]^{6-}$ (X = Cl, Br, I) carbido carbonyl clusters: Synthesis and characterization of the new $[H_{7-n}Ni_{32}C_4(CO)_{36}(CdX)]^{n-}$ (X = Cl, Br, I, N = 5, 6, 7), Inorg. Chim. Acta 362 (2009) 1239-1246.

[111] A. Bernardi, C. Femoni, M. C. Iapalucci, G. Longoni, F. Ranuzzi, S. Zacchini, P. Zanello, S. Fedi, Synthesis, Molecular Structure and Properties of the $[H_{6-n}Ni_{30}C_4(CO)_{34}(CdCl)_2]^{n-}$ (n = 3-6) Bimetallic Carbide Carbonyl Cluster: A Model for the Growth of Noncompact Interstitial Metal Carbides, Chem. Eur. J. 14 (2008) 1924-1934.

[112] M. Bortoluzzi, I. Ciabatti, C. Femoni, M. Hayatifar, M. C. Iapalucci, G. Longoni, S. Zacchini, Peraurated nickel carbide carbonyl clusters: the cationic $[Ni_6(C)(CO)_8(AuPPh_3)_8]^{2+}$ monocarbide and the $[Ni_{12}(C)(C_2)(CO)_{17}(AuPPh_3)_3]^{-}$ anion containing one carbide and one acetylide unit, Dalton Trans. 43 (2014) 13471-13475.

[113] I. Ciabatti, C. Femoni, M. C. Iapalucci, A. Ienco, G. Longoni, G. Manca, S. Zacchini, Intramolecular d^{10}-d^{10} Interactions in a $Ni_6C(CO)_9(AuPPh_3)_4$ Bimetallic Nickel-Gold Carbide Carbonyl Cluster, Inorg. Chem. 52 (2013) 10559-10565.

[114] N. Gupta, S. M. Gupta, S. K. Sharma, Carbon nanotubes: synthesis, properties and engineering applications, Carbon Nanolett. 29 (2019) 419-447.

[115] K. J. Kim, W.-R. Yu, J. H. Youk, J. Lee, Factors governing the growth of carbon nanotubes on carbon-based substrates, Phys. Chem. Chem. Phys. 14 (2012) 14041-14048.

[116] M. Moors, H. Amara, T. V. de Bocarmé, C. Bichara, F. Ducastelle, N. Kruse, J.-C. Charlier, Early Stages in the Nucleation Process of Carbon Nanotubes, ACS Nano 3 (2009) 511-516.

[117] J. Lahiri, T. Miller, L. Adamska, I. I. Oleynik, M. Batzill. Graphene Growth on Ni(111) by Transformation of a Surface Carbide, Nano Lett. 11 (2011) 518-522.

[118] C. Cesari, T. Funaioli, B. Berti, C. Femoni, M. C. Iapalucci, F. M. Vivaldi, S. Zacchini, Atomically Precise Ni-Pd Alloy Carbonyl Nanoclusters: Synthesis, Total Structure, Electrochemistry, Spectroelectrochemistry, and Electrochemical Impedance Spectroscopy, Inorg. Chem. 60 (2021) 16713-16725.

[119] F. Calderoni, F. Demartin, F. Fabrizi de Biani, C. Femoni, M. C. Iapalucci, G. Longoni, P. Zanello, Electron-Sink Behaviour of the Carbonylnickel Clusters $[Ni_{32}C_6(CO)_{36}]^{6-}$: Synthesis ad Characterization of the Anions $[Ni_{32}C_6(CO)_{36}]^{n-}$ (n = 5-10) and $[Ni_{38}C_6(CO)_{42}]^{n-}$ (n = 5-9) and Crystal Structure of $[PPh_3Me]_6[Ni_{32}C_6(CO)_{36}]\cdot 4MeCN$, Eur. J. Inorg. Chem. (1999) 663-671.

[120] D. Collini, F. Fabrizi de Biani, D. S. Dolzhnikov, C. Femoni, M. C. Iapalucci, G. Longoni, C. Tiozzo, S. Zacchini, P. Zanello, Synthesis, Structure, and Spectroscopic Characterization of $[H_{8-n}Rh_{22}(CO)_{35}]^{n-}$ (n = 4, 5) and $[H_2Rh_{13}(CO)_{24}\{Cu(MeCN)\}_2]^-$ Clusters: assessment of CV and DPV As Techniques to Circumstantiate the Presence of Elusive Hydride Atoms, Inorg. Chem. 50 (2011) 2790-2798.

[121] H. Kreissl, J. Jin, S.-H. Lin, D. Schüette, S. Störte, N. Levin, B. Chaudret, A. J. Vorholt, A. Bordet, W. Leiner, Commercial $Cu_2Cr_2O_5$ Decorated with Iron Carbide Nanoparticles as a Multifunctional Catalyst for Magnetically Induced Continuous-Flow Hydrogenation of Aromatic Ketones, Angew. Chem. Int. Ed. 60 (2021) 26639-26646.